Optomechanical Integrated Circuits for Efficient Microwave-to-Optical Transduction

I-Tung Chen
Advisor: Prof. Mo Li
Department of Electrical & Computer Engineering
University of Washington, Seattle, WA

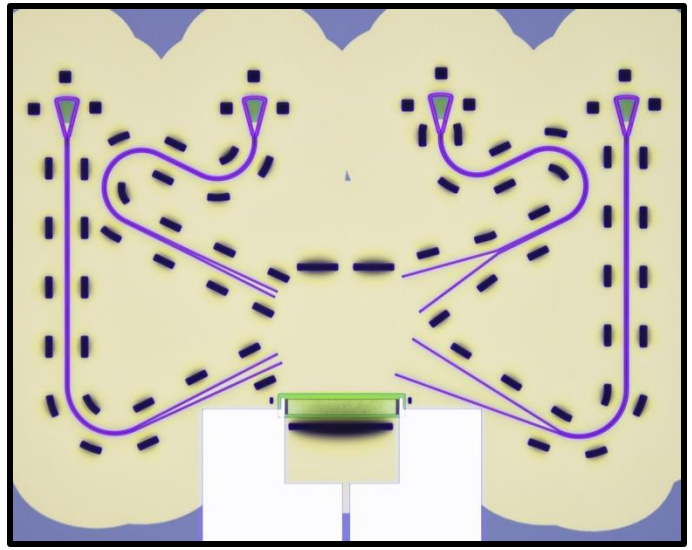

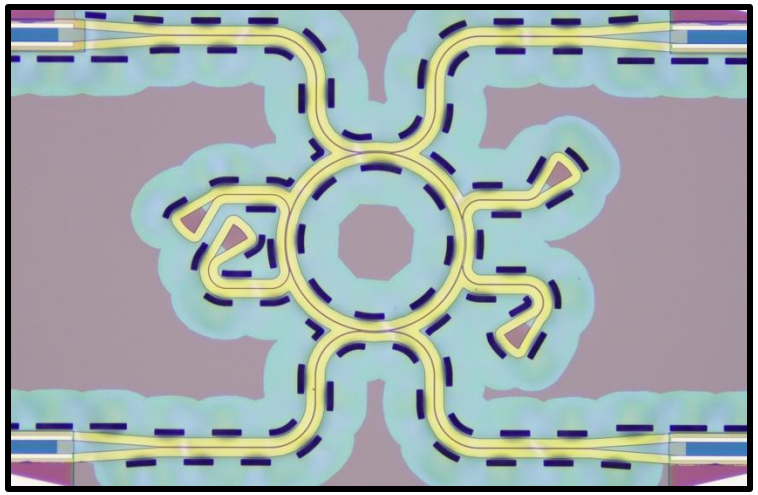

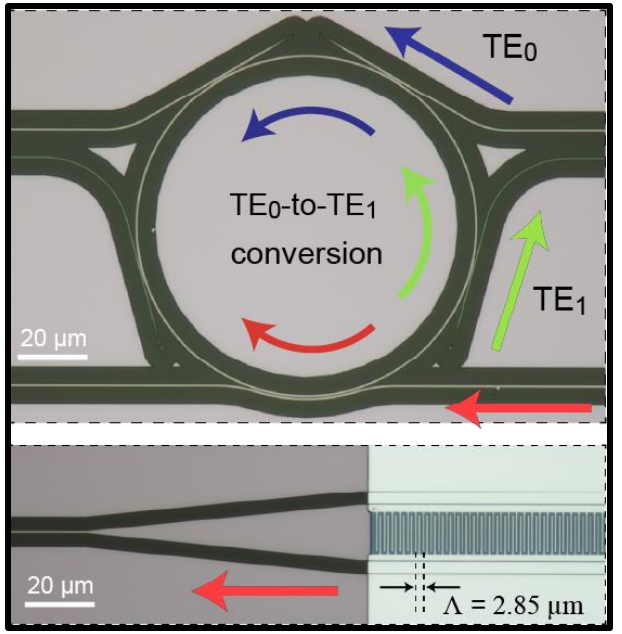

Motivation for microwave-to-optical transduction

November 2024, IBM Quantum

December 2024, Google Quantum AI

Systems	N_{qubits}	$F_{single-qb}$	F_{two-qb}
IBM Quantum	156	$\sim 99.96\%$	
Google quantum AI	105		
	↓ Enormous gap!		
Practical quantum advantage* (M. Beverland et al, 2022)	$>10^6$	$> 99.999\%$	

*Depending on the type of error correction scheme used but more or less in this range

Optical interconnection for qubits

Many qubits in one fridge (a thousand)

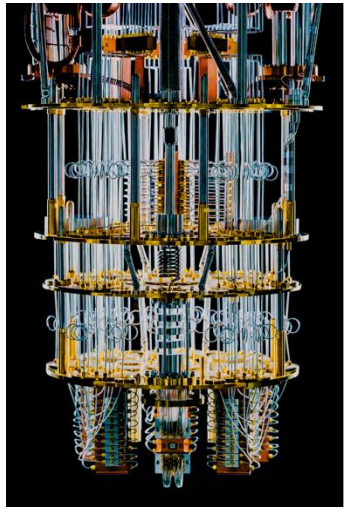

IBM Quantum computer at Yorktown Heights, Nov. 8, 2021. (PHOTOGRAPH BY BENEDICT EVANS)

Limitations:
Coaxial cables[1]
Cooling powers[2]

Many qubits in many fridges (ten thousands)

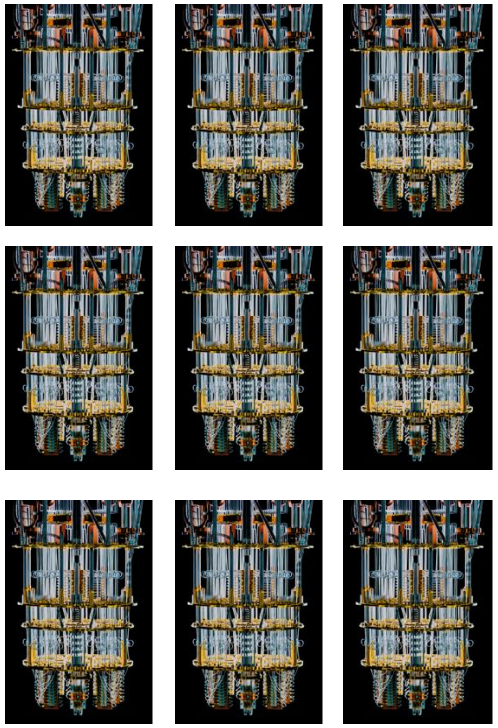

Not enough

Optical interconnected qubits (millions)

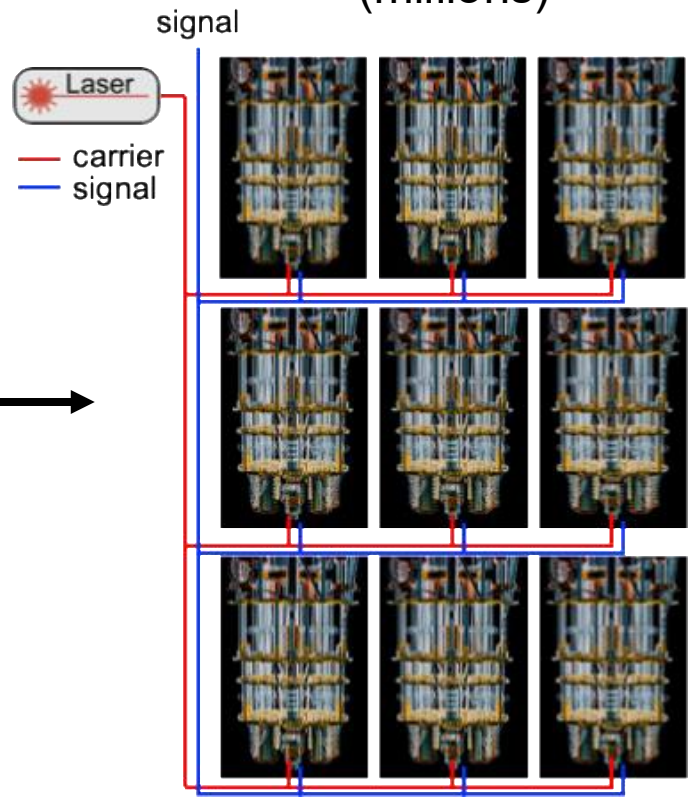

Optical fibers:
Dilfridge's cooling power at MXC~ one million fibers' passive heat load[3]

This requires microwave-to-optical transduction!

[1] Kim, Y. et al. Nature 618, 500–505 (2023)
[2] S. Joshi and S. Moazeni, *J. of Lightwave Technology*, vol. 42, no. 1, pp. 166-175, (2024)
[3] Lecocq, F., et al. *Nature* **591**, 575–579 (2021).

Overview

- **Introduction and examples of microwave-to-optical transductions**
  - **Traveling waves:** acousto-optics through phase-matching condition
  - **Standing waves:** cavity-optomechanics through moving boundary and photoelastic effects
- **Optomechanical integrated circuits (OMIC)** for microwave-to-optical transduction

Acousto-optics frequency shifter (AOFS)

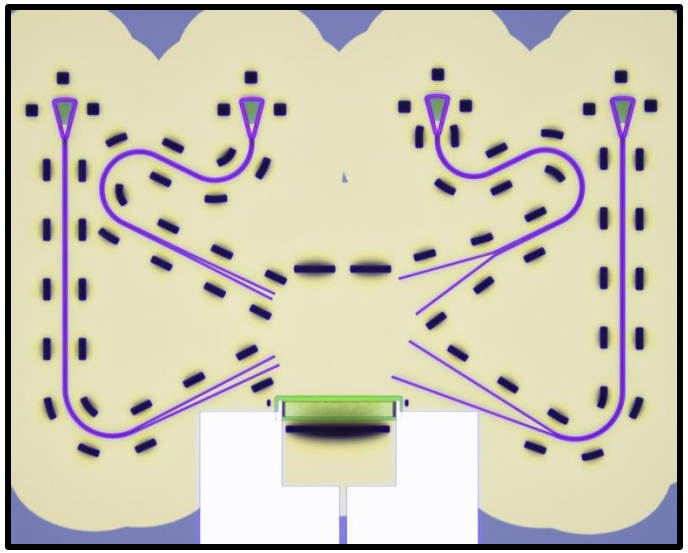

N. S. Yama*, I.-T. Chen* et al., Advanced Materials (2023)

Microwave-to-optical transduction

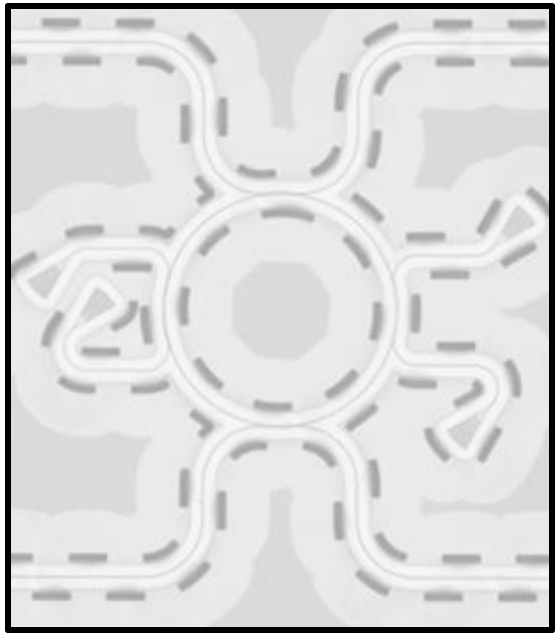

I.-T. Chen et al., Nat. Commun (2023)

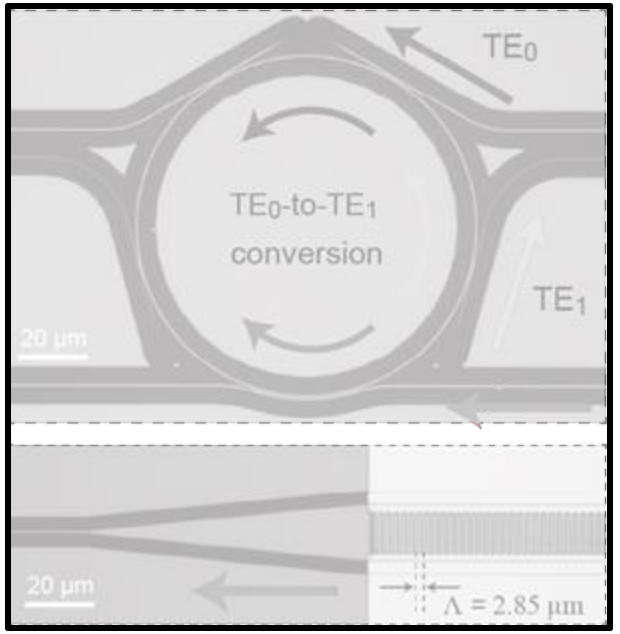

I.-T. Chen et al., submitted (2025)

Introduction to microwave-to-optical transduction

One of the simplest ways to convert microwave signal to optical frequency (classical)

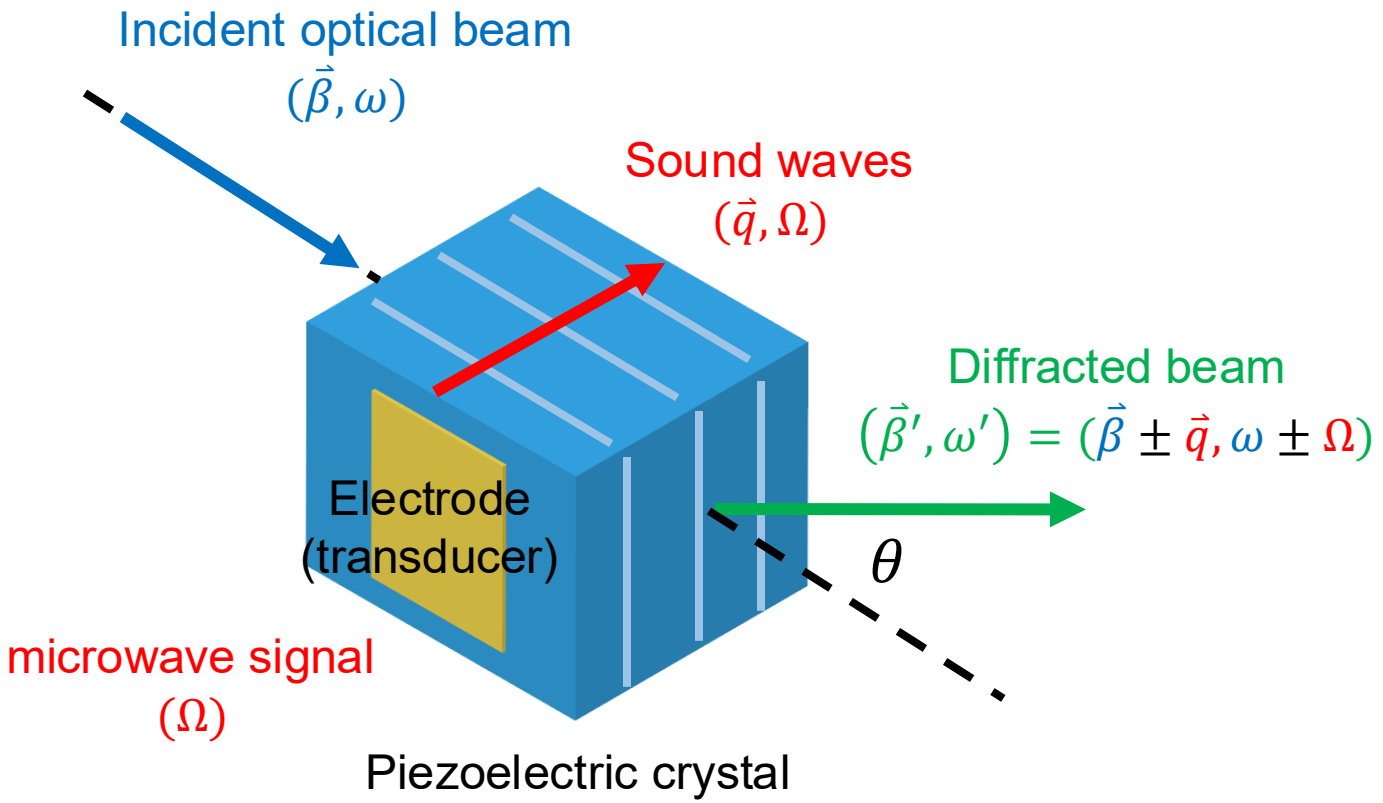

Brillouin scattering,
which satisfy the phase-matching condition

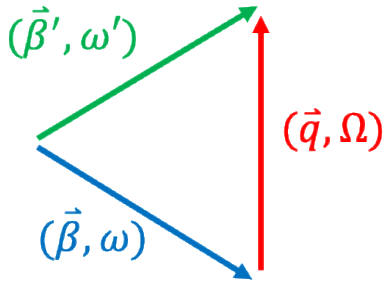

$$(\vec{\beta}', \omega') = (\vec{\beta} \pm \vec{q}, \omega \pm \Omega)$$

(+): Anti-Stokes: absorbs phonon
(−): Stokes: emits phonon

Microwave → Sound (phonons) → Optical signal

Other methods: electro-optics[1]. Here, we choose phonon because of its high conversion efficiency and scalability

[1] Sahu, R. Science 380, 718–721 (2023).

Brillouin scattering: an example

Boron-doped Gallium Phosphide (BGaP): Acousto-Optics Frequency Shifter

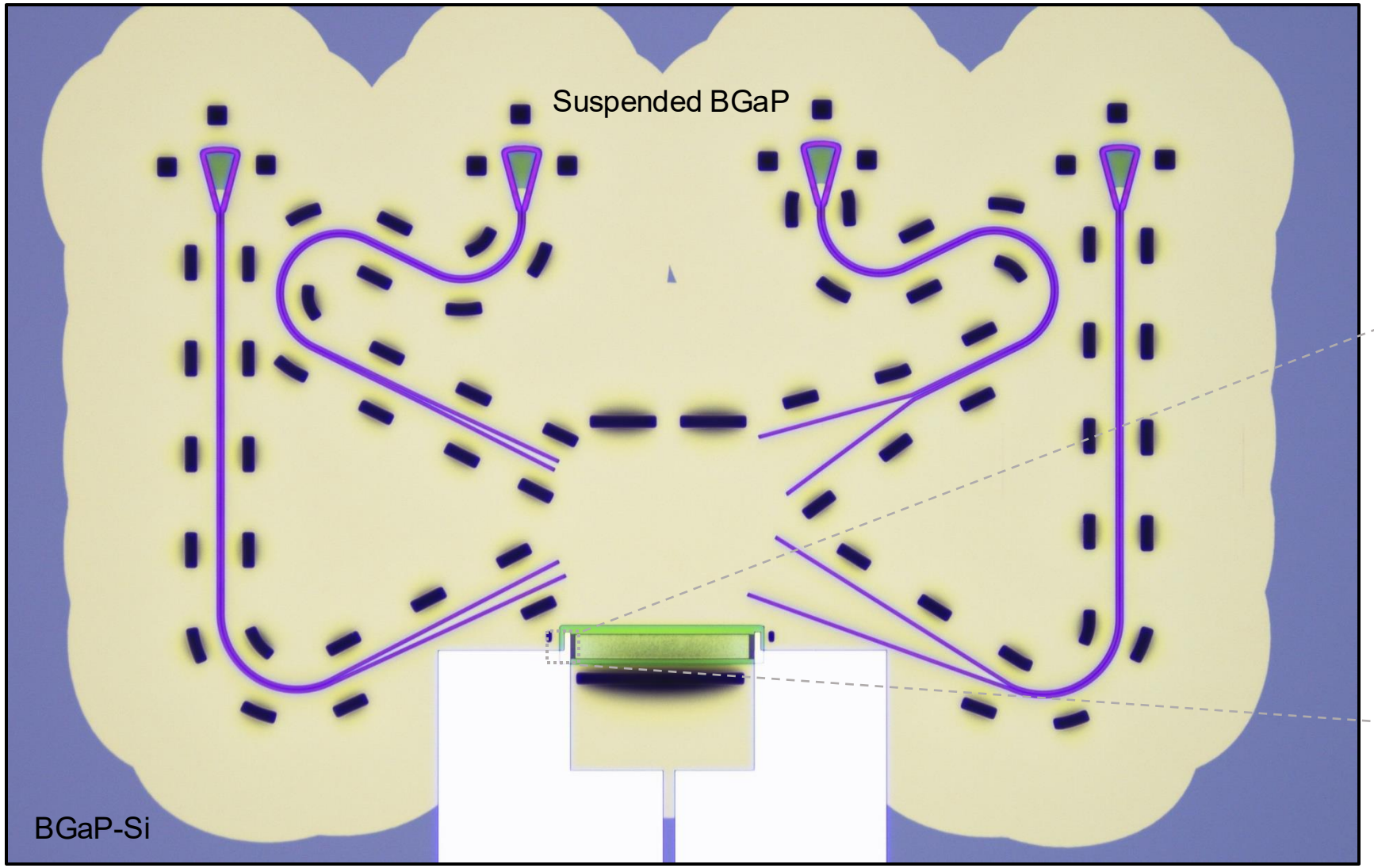

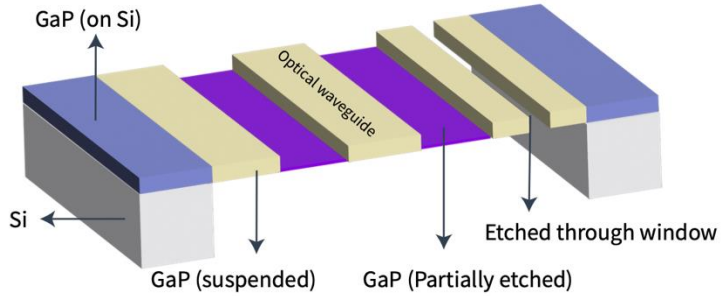

IDT on ZnO to excite acoustic waves

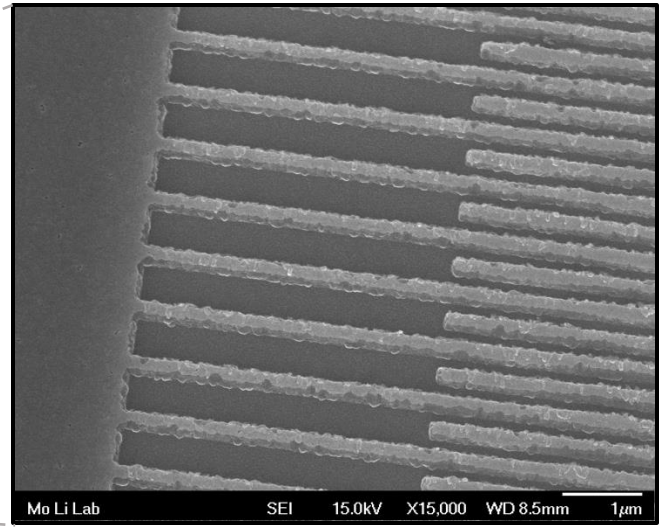

BGaP: weakly piezoelectric

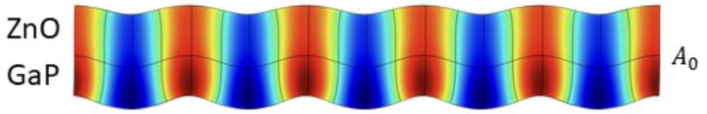

Acoustic wave profile

N. S. Yama*, I.-T. Chen* et al., Advanced Materials, (2023). *Equal contribution authors

Brillouin scattering: heterodyne measurement technique

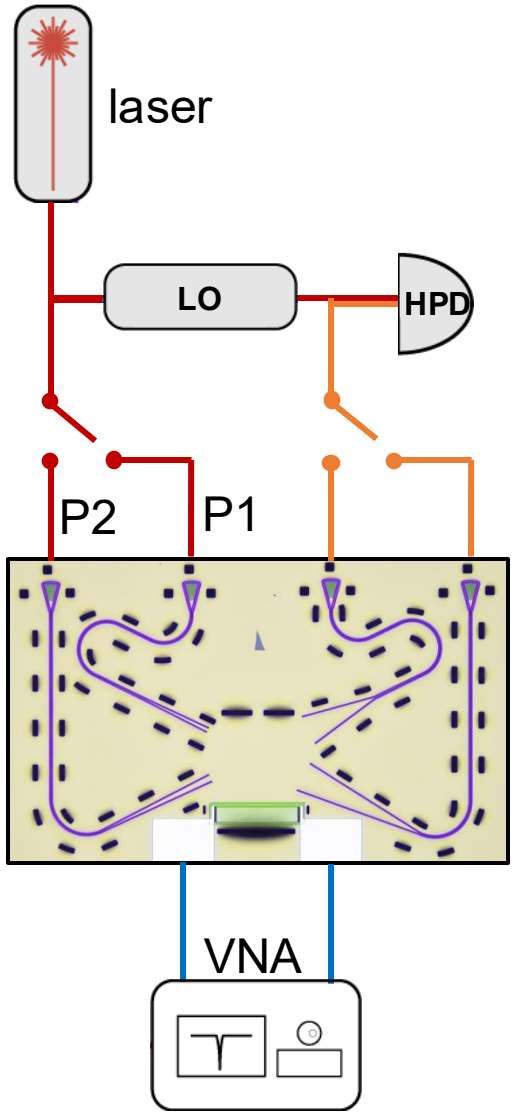

Anti-Stokes scattering $k_{in} + q = k_{as}$

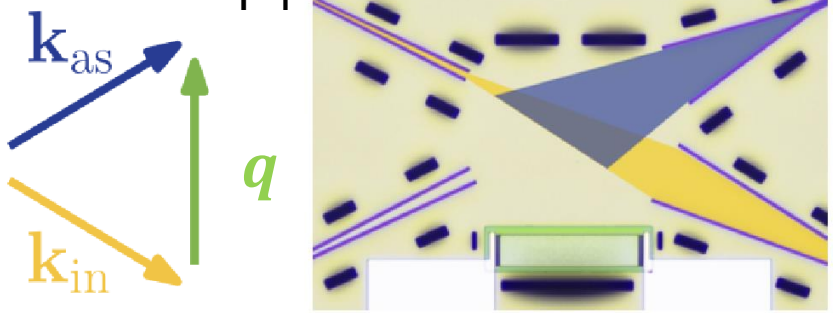

Stokes scattering $k_{in} - q = k_s$

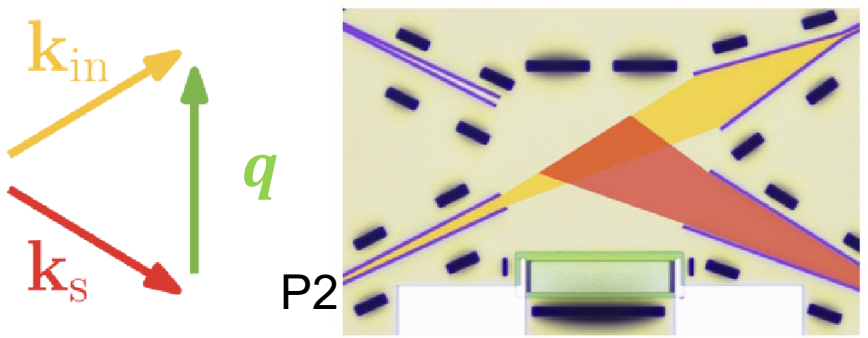

Heterodyne measurement

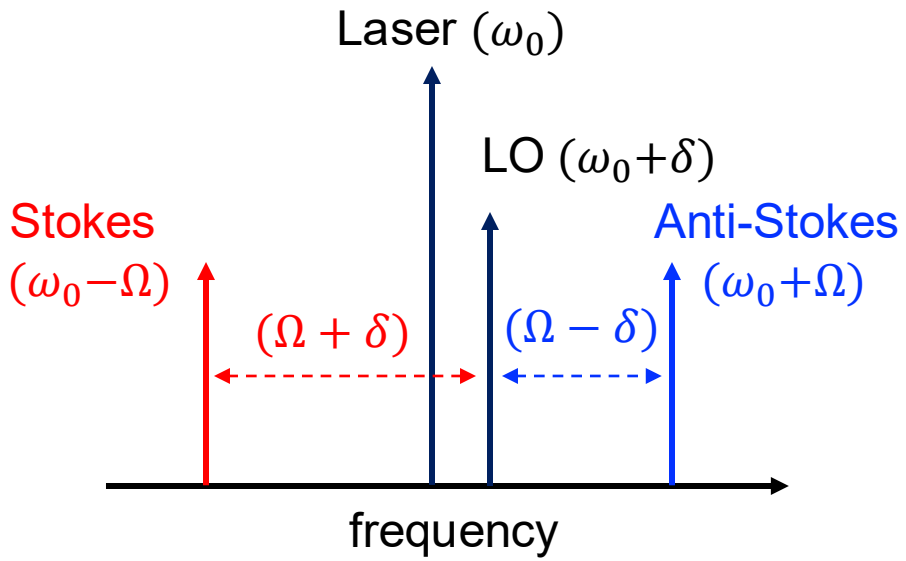

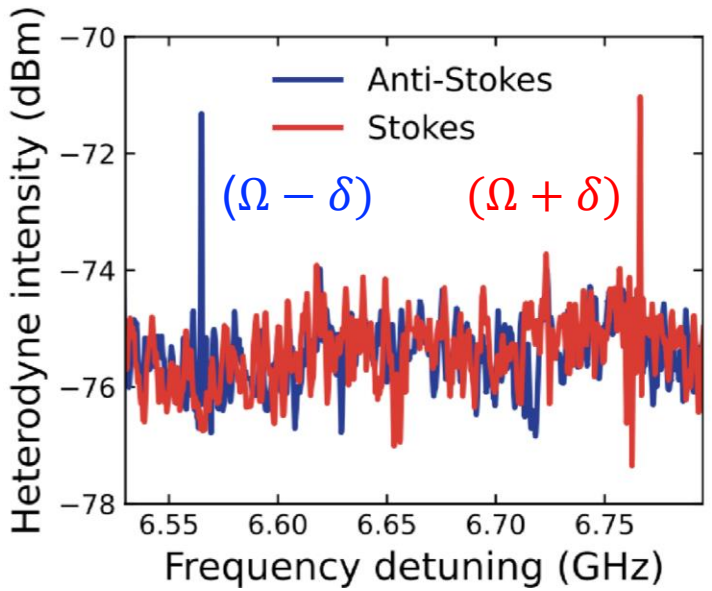

Microwave → Sound (phonons) → Optical signal

N. S. Yama*, I.-T. Chen* et al., Advanced Materials, (2023). *Equal contribution authors

How to enhance the photon-phonon interaction?

Microwave → Sound (phonons) → Optical signal (photons)

Traveling waves:
phase-matching condition

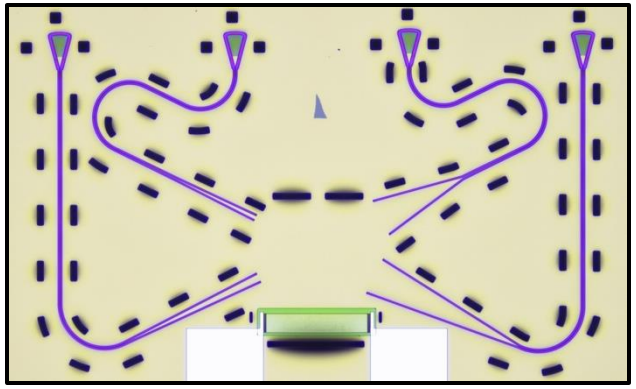

- Requires large photon-phonon interaction area
- Requires high microwave power for 100% mode conversion efficiency

Standing waves:
moving boundary and photoelastic effect

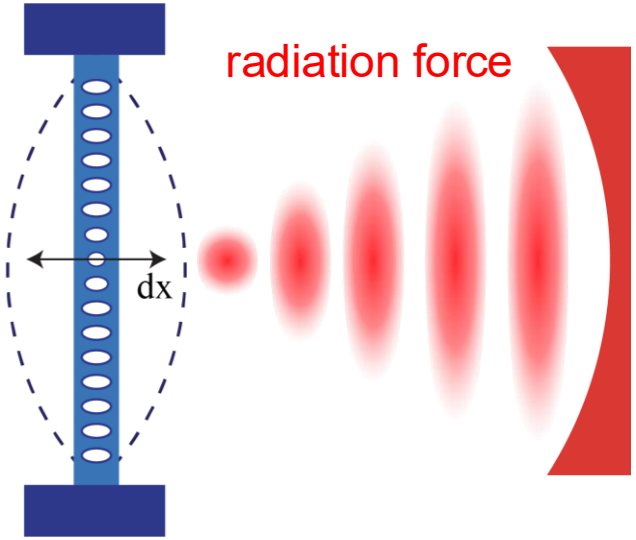

- Cavity-optomechanics
- Cavity-confined optical and acoustic modes

Cavity-optomechanics mw-to-optical transduction

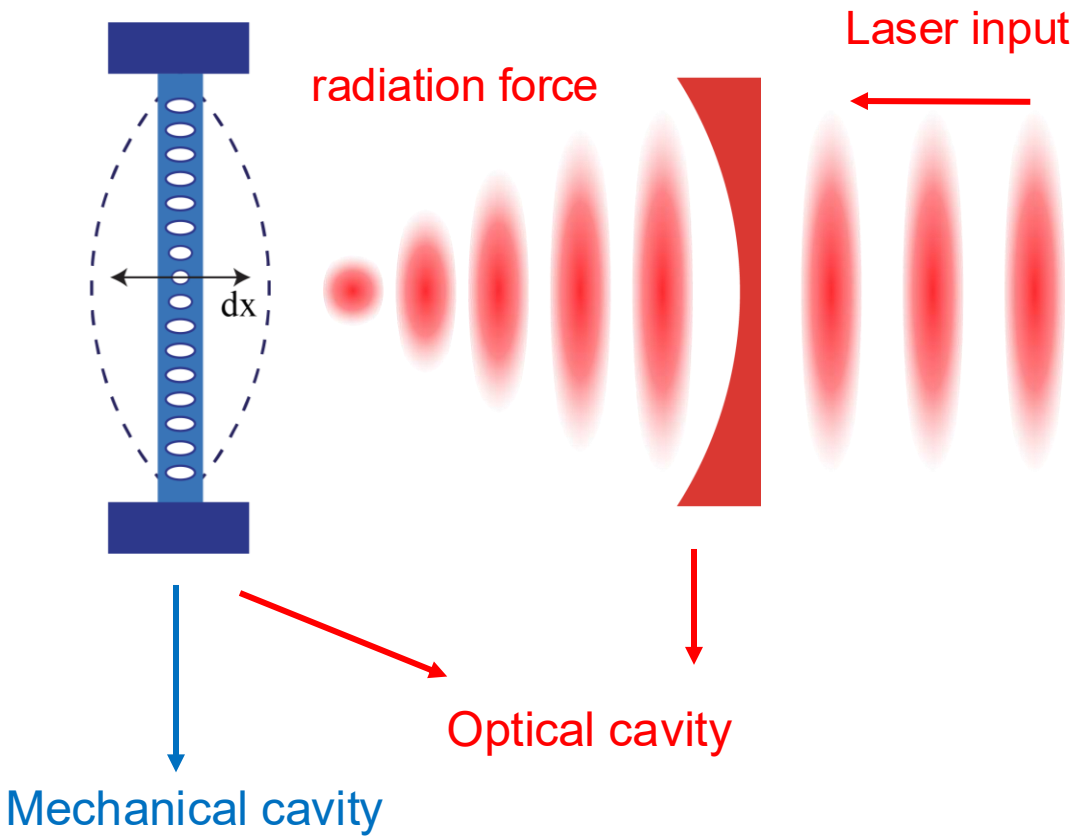

"The radiation pressure of light in the cavity causes the material to deform, which shifts the cavity's resonant frequency."

$$\boldsymbol{\omega_{cav}(x)} \approx \omega_{cav} + x\frac{\partial \omega_{cav}}{\partial x} + \cdots$$

$$\hat{H}_{OM} = \hbar\Omega\hat{b}^{\dagger}\hat{b} + \hbar\boldsymbol{\omega_{cav}(x)}\hat{a}^{\dagger}\hat{a} = \hbar\Omega\hat{b}^{\dagger}\hat{b} + \hbar(\omega_{cav} - G\hat{x}\,)\hat{a}^{\dagger}\hat{a}$$

where the coupling coefficient $G \equiv -\frac{\partial \omega_{cav}}{\partial x}, \hat{x} = x_{ZPF}(\hat{b} + \hat{b}^{\dagger})$

$$\hat{H}_{int} = \hbar g(\,\hat{b} + \hat{b}^{\dagger})\hat{a}^{\dagger}\hat{a}$$

An ***optomechanical cavity***

What is "g" exactly?

M. Aspelmeyer et al, Cavity Optomechanics, 2013

Optomechanical coupling rate g_{om}

Photonic mode

Phononic mode

Photoelastic effect (PE)

Moving boundary effect (MB)

Silicon optomechanical cavity

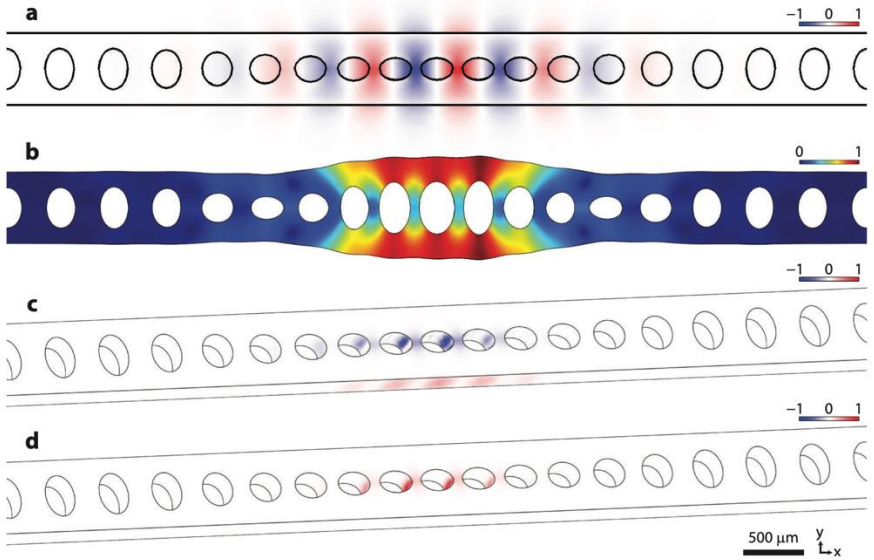

$$g_{OM} = g_{PE} + g_{MB}$$

$$g_{PE} = \left\langle \boldsymbol{E} \left| \frac{d\varepsilon_{PE}}{du} \right| \boldsymbol{E} \right\rangle_V \propto (\varepsilon \cdot p\boldsymbol{S} \cdot \varepsilon) \propto n^4$$

$$g_{MB} = \left\langle \boldsymbol{E} \left| \frac{d\varepsilon_{MB}}{du} \right| \boldsymbol{E} \right\rangle_S \propto (\Delta\varepsilon' \left|\boldsymbol{E}_{\parallel}\right|^2 - \Delta\varepsilon'^{-1} \left|\boldsymbol{D}_{\perp}\right|^2)$$

PE: Bulk effect
- Photoelastic coefficient tensor (p)
- Strain tensor ($\boldsymbol{S}$)

MB: Surface effect
- tangential electric field ($\boldsymbol{E}_{\parallel}$)
- normal displacement field ($\boldsymbol{D}_{\perp}$)

How to use this to convert microwave signal to optical?

Chan, Jasper (2012) *Laser Cooling of an Optomechanical Crystal Resonator to Its Quantum Ground State of Motion.* Dissertation (Ph.D.), California Institute of Technology. doi:10.7907/ZRFK-2W24.

Cavity-optomechanics mw-to-optical transduction

By H_{int} linearization ($\hat{a} \rightarrow \bar{\alpha} + \delta\hat{a}$) and rotating-wave approximation at the lab frame (discarding 2Ω terms)

$$\hat{H}_{red} = \hbar g(\delta\hat{a}\hat{b}^{\dagger} + \delta\hat{a}^{\dagger}\hat{b})$$

At red detuning $\Delta = -\Omega$

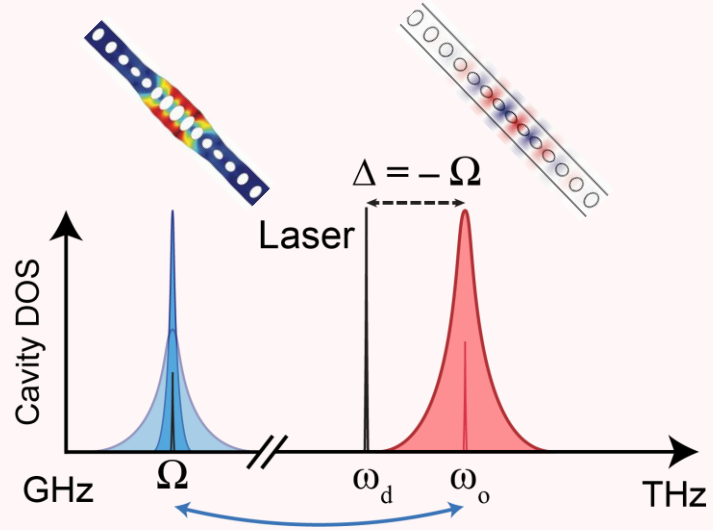

microwave-to-optical transduction

Sound (phonons) → Optical signal (photons)

Microwave-frequency *photons* from superconducting qubits $\hat{c}$

Electromechanical transducer

Piezoelectric material

Microwave mechanical modes $\hat{b}$

Red detuned laser pump

$$\hat{H}_{red} = \hbar g(\delta\hat{a}\hat{b}^{\dagger} + \delta\hat{a}^{\dagger}\hat{b})$$

in an optomechanical cavity

Terahertz optical modes $\hat{a}$

Cavity-optomechanics microwave-to-optical transduction

Optomechanical cavity (OMC)

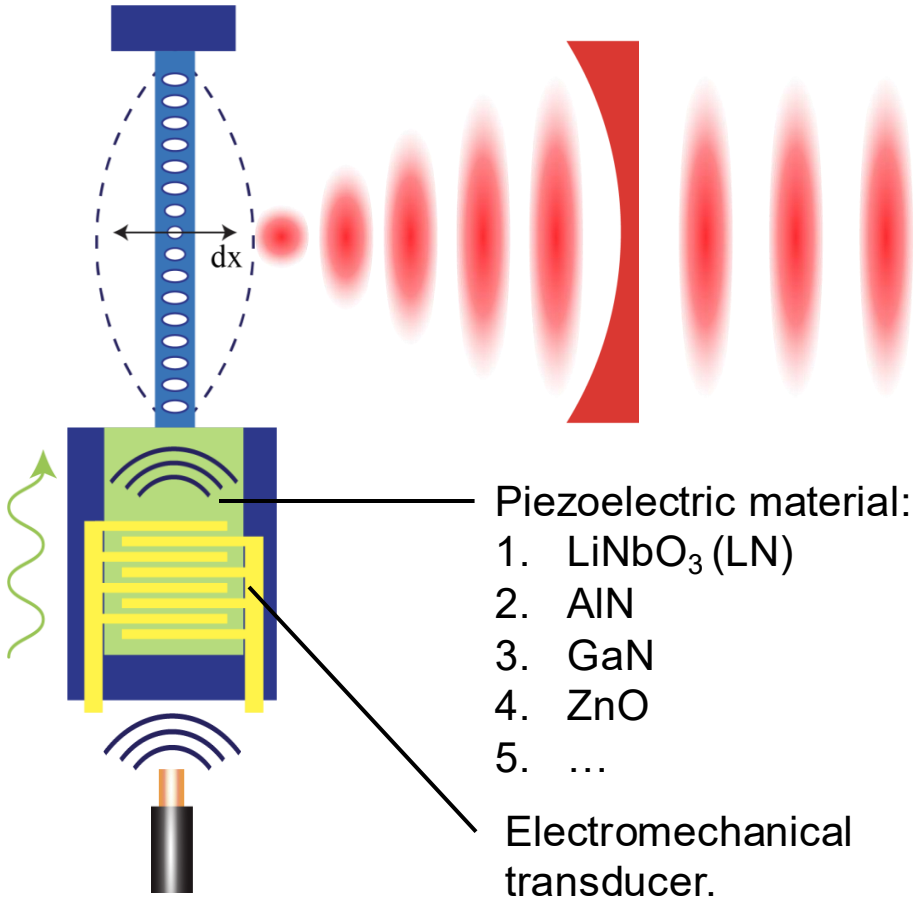

Piezoelectric material:

1. $LiNbO_3$ (LN)
2. AlN
3. GaN
4. ZnO
5. …

Electromechanical transducer.

OMC + Piezoelectric material: $LiNbO_3$

W. Jiang et al., Nat comm (2020)

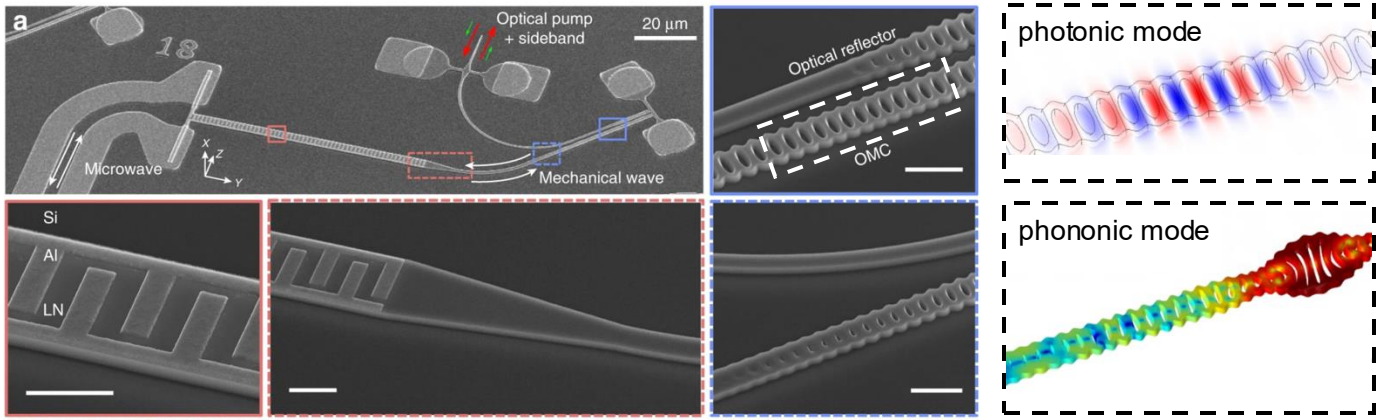

$LiNbO_3$-on-Si

M. J. Weaver et al., Nat. Nanotech. (2023)

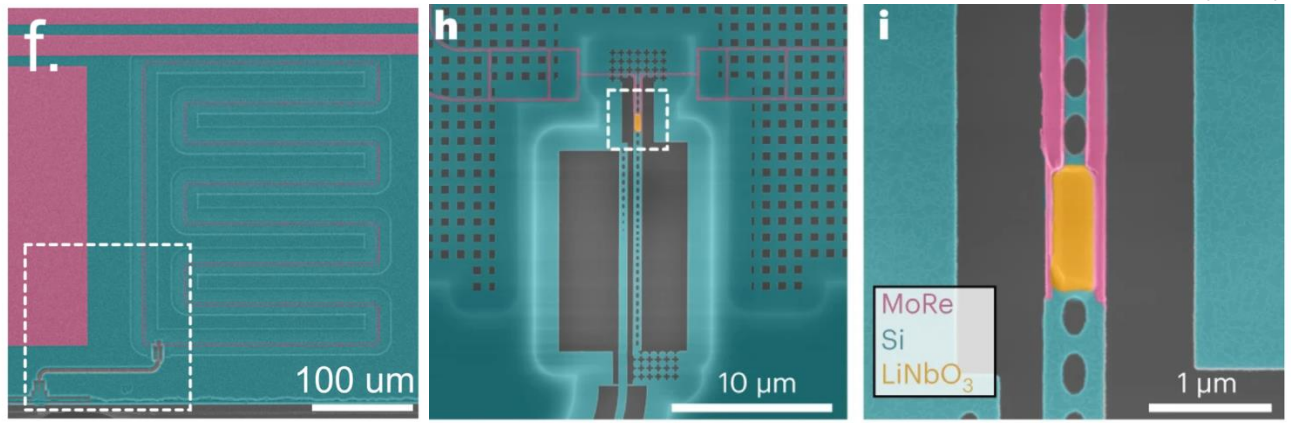

microwave photonic mode

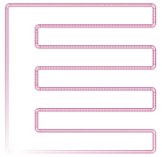

phononic mode

optical photonic mode

Overview

- Introduction and examples of microwave-to-optical transductions
  - **Traveling waves:** acousto-optics through phase-matching condition
  - **Standing waves:** cavity-optomechanics through moving boundary and photoelastic effects
- Optomechanical integrated circuits (OMIC) for m-to-o transduction

Acousto-optics frequency shifter (AOFS)

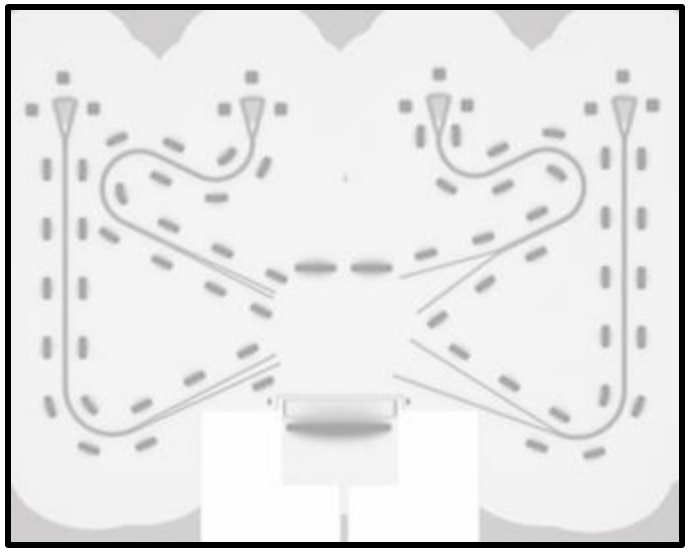

N. S. Yama*, I.-T. Chen* et al., Advanced Materials (2023)

Microwave-to-optical transduction

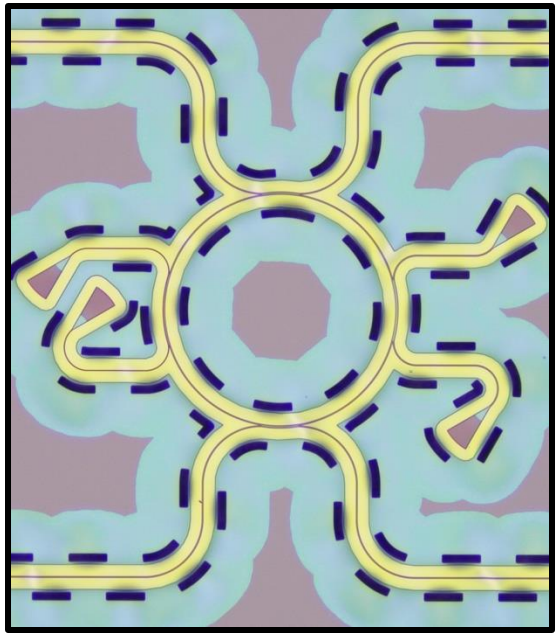

I.-T. Chen et al., Nat. Commun. (2023)

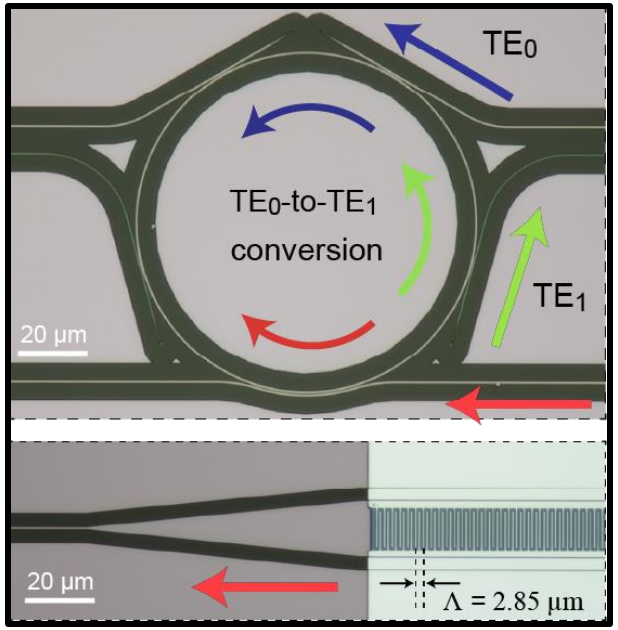

I.-T. Chen et al., submitted (2025)

Optomechanical Integrated Circuit Coupling Rate g_{OMIC}

Standing waves:
Cavity-optomechanics
Two-mode coupling: $\hat{a}$ and $\hat{b}$

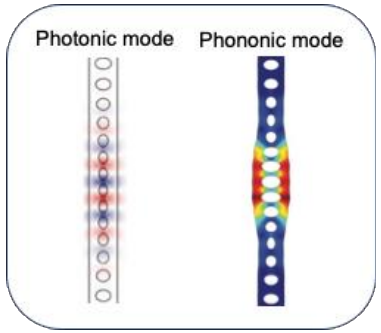

$$g_{OM} = g_{PE} + g_{MB}$$

Traveling waves:
Brillouin scattering
Three-mode coupling: $\hat{a}_0$, $\hat{a}_1$ and $\hat{b}$

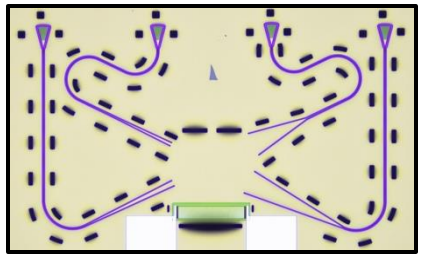

$$\vec{\beta}_0 \pm \vec{q} = \vec{\beta}_1$$

$$\omega_0 \pm \Omega = \omega_1$$

Cavity-optomechanics | Brillouin Scattering

$$= g_{OMIC} = \underbrace{\left(\left\langle \boldsymbol{E_0} \left| \frac{d\varepsilon_{PE}}{du} \cdot \boldsymbol{u} \right| \boldsymbol{E_1} \right\rangle_V + \left\langle \boldsymbol{E_0} \left| \frac{d\varepsilon_{MB}}{dx} \cdot \boldsymbol{u} \right| \boldsymbol{E_1} \right\rangle_S \right)}_{\text{PE} \qquad\qquad \text{MB}} \cdot \underbrace{exp^{-i\left(\vec{\beta}_0 \pm \vec{q} \mp \vec{\beta}_1\right)r} \cdot exp^{-i(\omega_0 \pm \Omega \mp \omega_1)t}}_{\text{Phase-matching condition}}$$

Phonon → photon when phase-matching conditions is satisfied

I. -T. Chen et al, Nat. Comm. 14, 7594 (2023)
I. -T. Chen et al., submitted (2025)

Building block for interconnecting qubits

$$\hat{H}_{int} = \hbar g_{OMIC}{}' \left(\hat{a}_0{}^{\dagger} \hat{a}_1 \hat{b}^{\dagger} + \hat{a}_0 \hat{a}_1{}^{\dagger} \hat{b} \right) exp^{-i\left(\vec{\beta}_0 \pm \vec{q} \mp \vec{\beta}_1\right) r} \cdot exp^{-i(\omega_0 \pm \Omega \mp \omega_1) t} + h.c.,$$

When the PMC are satisfied: $\vec{\beta}_0 + \vec{q} = \vec{\beta}_1$

- When laser drives: $\hat{a}_0 \rightarrow \langle \hat{a}_0 \rangle$,

$\hat{H}_{red} = \hbar G_0 (\hat{a}_1 \hat{b}^{\dagger} + \hat{a}_1^{\dagger} \hat{b})$ $\quad G_0 = g_{OMIC} \langle \hat{a}_0 \rangle$

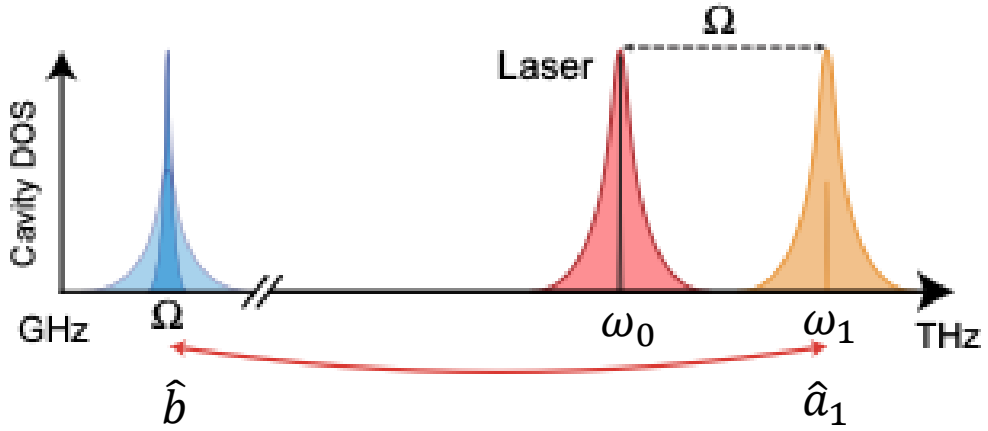

microwave phonon ↔ optical transduction

- When laser drives: $\hat{a}_1 \rightarrow \langle \hat{a}_1 \rangle$,

$\hat{H}_{blue} = \hbar G_1 (\hat{a}_0^{\dagger} \hat{b}^{\dagger} + \hat{a}_0 \hat{b})$ $\quad G_1 = g_{OMIC} \langle \hat{a}_1 \rangle$

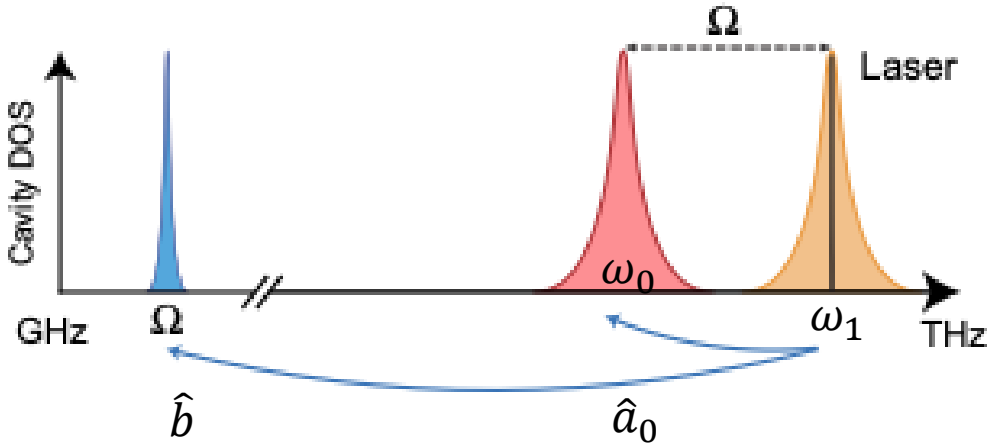

microwave phonon ↔ optical entanglement

By selecting a drive optical mode →
select transduction or entanglement generation

I. -T. Chen et al, Nat. Comm. 14, 7594 (2023)
I. -T. Chen et al., submitted (2025)

Realizing Optomechanical Integrated Circuits (OMIC)

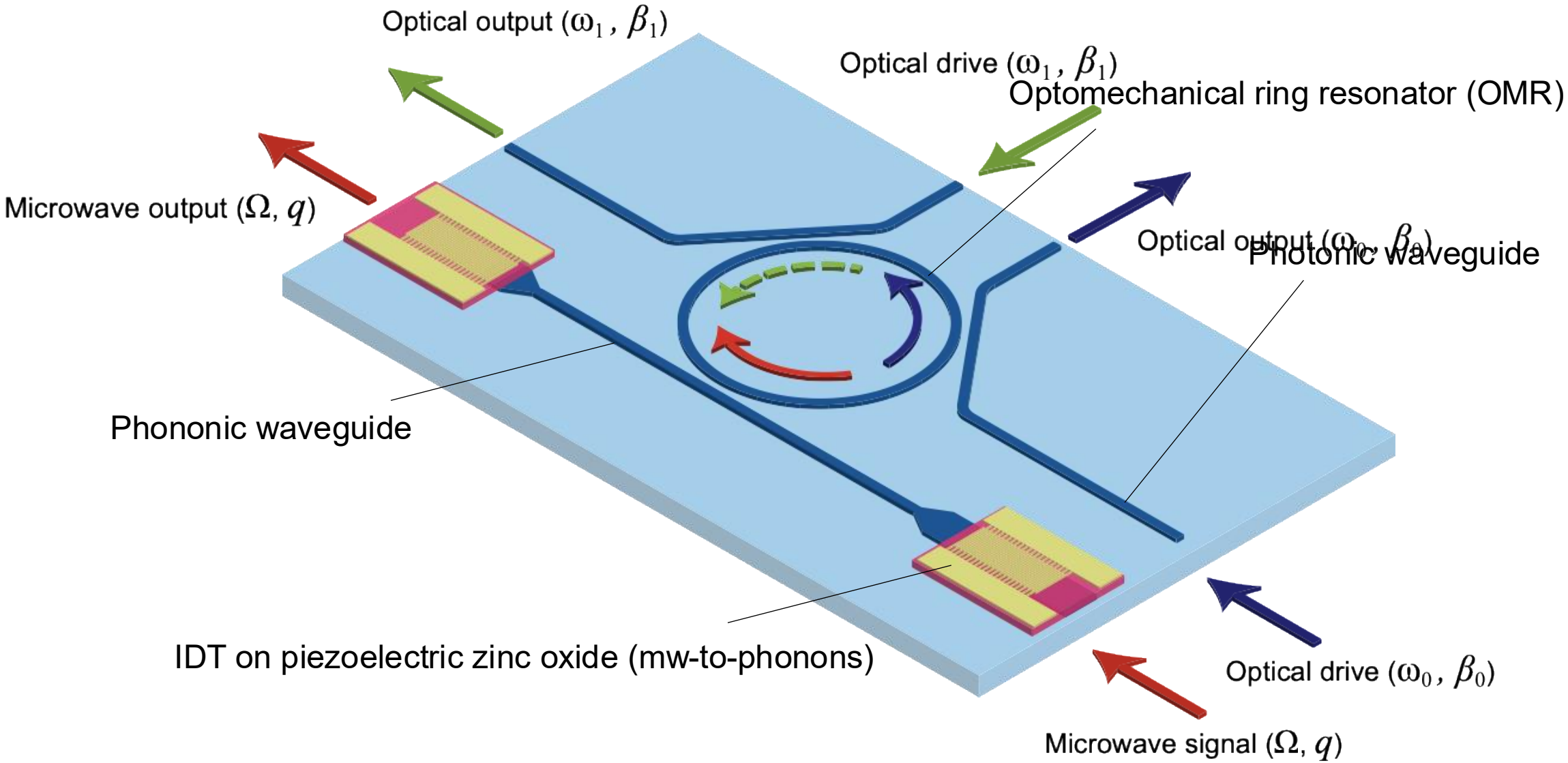

$$\hat{H}_{int} = \hbar G_1 (\hat{a}_1^\dagger \hat{a}_1 \hat{b}^\dagger + \hat{a}_1^\dagger \hat{a}_1 \hat{b})$$

I. -T. Chen et al, Nat. Comm. 14, 7594 (2023)
I. -T. Chen et al., submitted (2025)

Material requirements

Material requirements for optomechanical integrated circuits

- Acoustic wave guiding: low acoustic velocity (v)
- Optical wave guiding: high refractive index (n)
- Strong optomechanical interaction: high photoelastic coefficient (p)
- Can convert microwave signal to acoustic wave: piezoelectricity

Acousto-optic figure-of-merit: $M_2 = \frac{p^2 n^6}{\rho v^3}$

$(\times 10^{-15})$

	k_{em}^2 (%)	n (1.55 μm)	p_{ij}	ρ (g/cm^3)	v_s (m/s)	$\mathcal{M}_2$(s^3kg^{-1})
AlN	7.2	2.19	$p_{11} = -0.1$	3.26	5760	1.7
GaAs	0.38	3.37	$p_{11} = -0.16$	5.32	4726	66.7
GaN	1.3	2.31	$p_{11} = -0.09$	6.15	3941	3.26
GaP	0.2	3.05	$p_{11} = 0.151$ [32]	4.13	4100	64.5
$LiNbO_3$	17.2	2.21	$p_{31} = 0.172$ [32]	4.64	3978 (Y-cut)	11.8
Si*	0	3.47	$p_{11} = -0.095$ (RT) -0.160 $(5K)$	2.33	5845	36.1 60.6
ZnO	3.3	1.92	$p_{11} = -0.2$	5.61	3500	8.3

Experimental realization: OMIC on BGaP

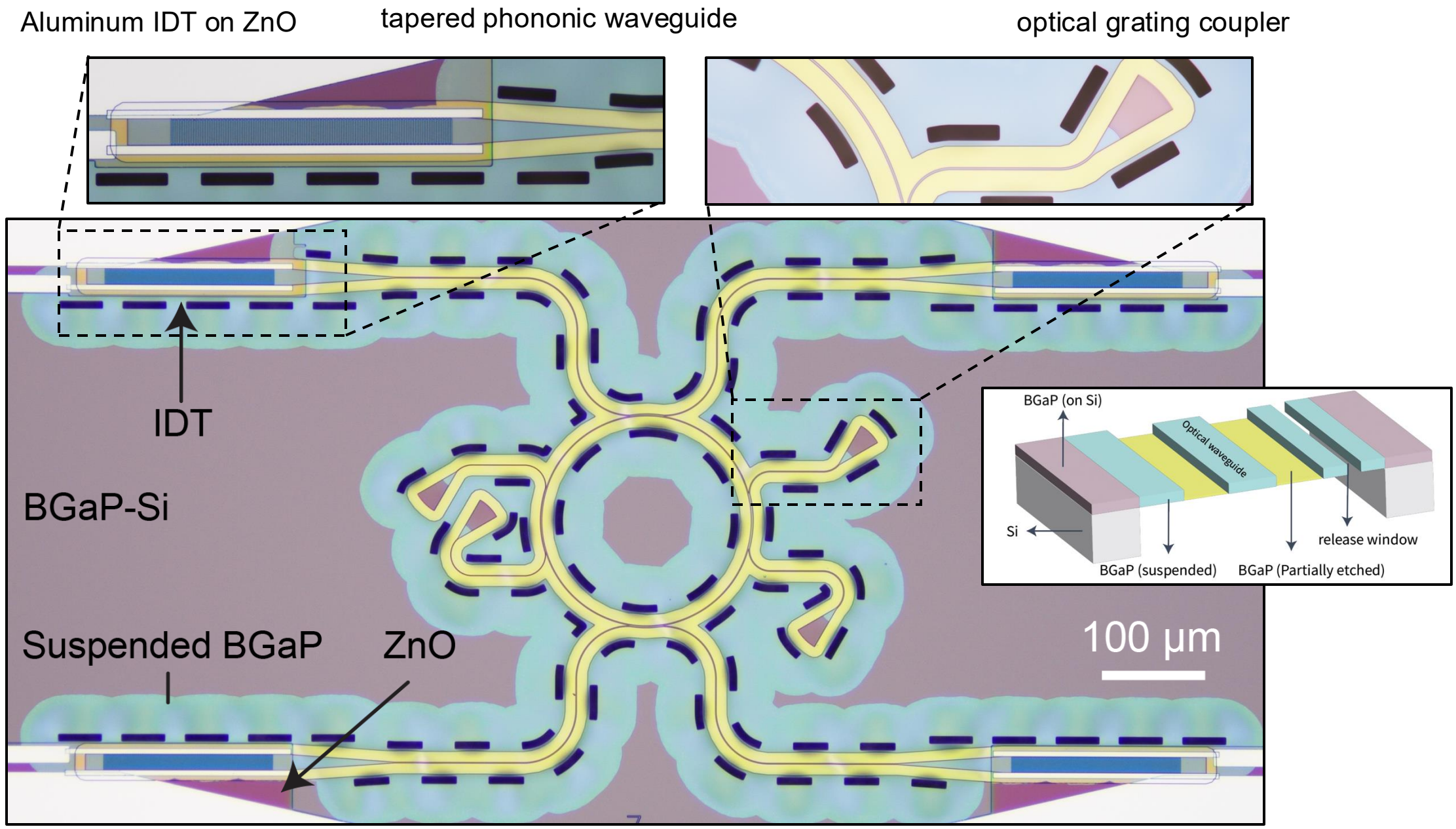

I. -T. Chen et al, Nat. Comm. 14, 7594 (2023)

Phase-matching condition in OMR

Three modes propagates in OMIC

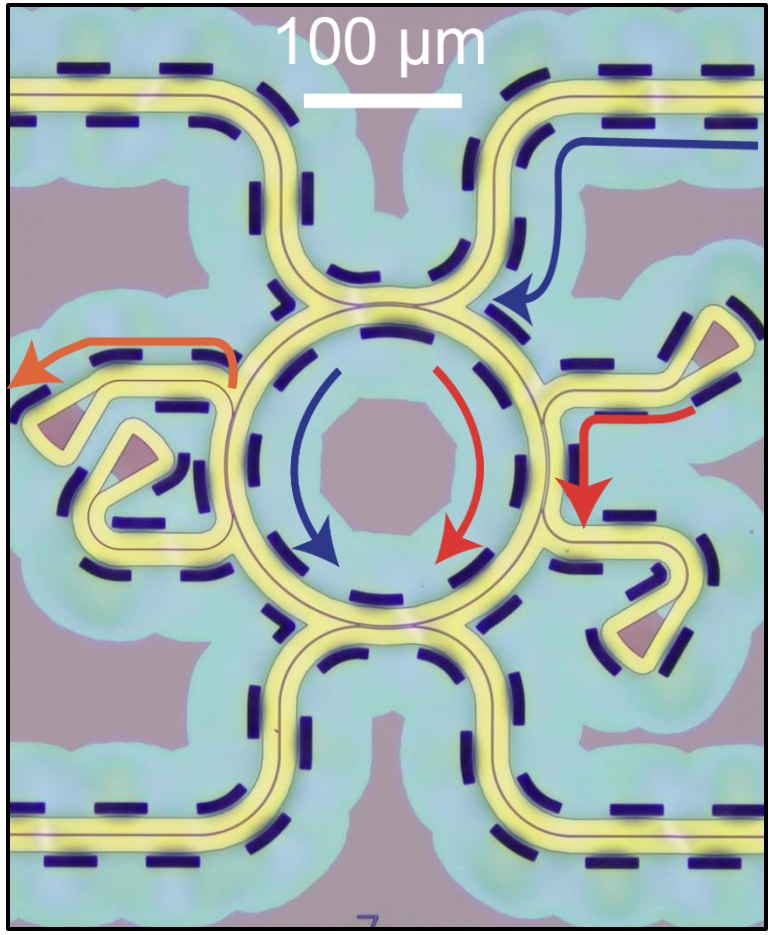

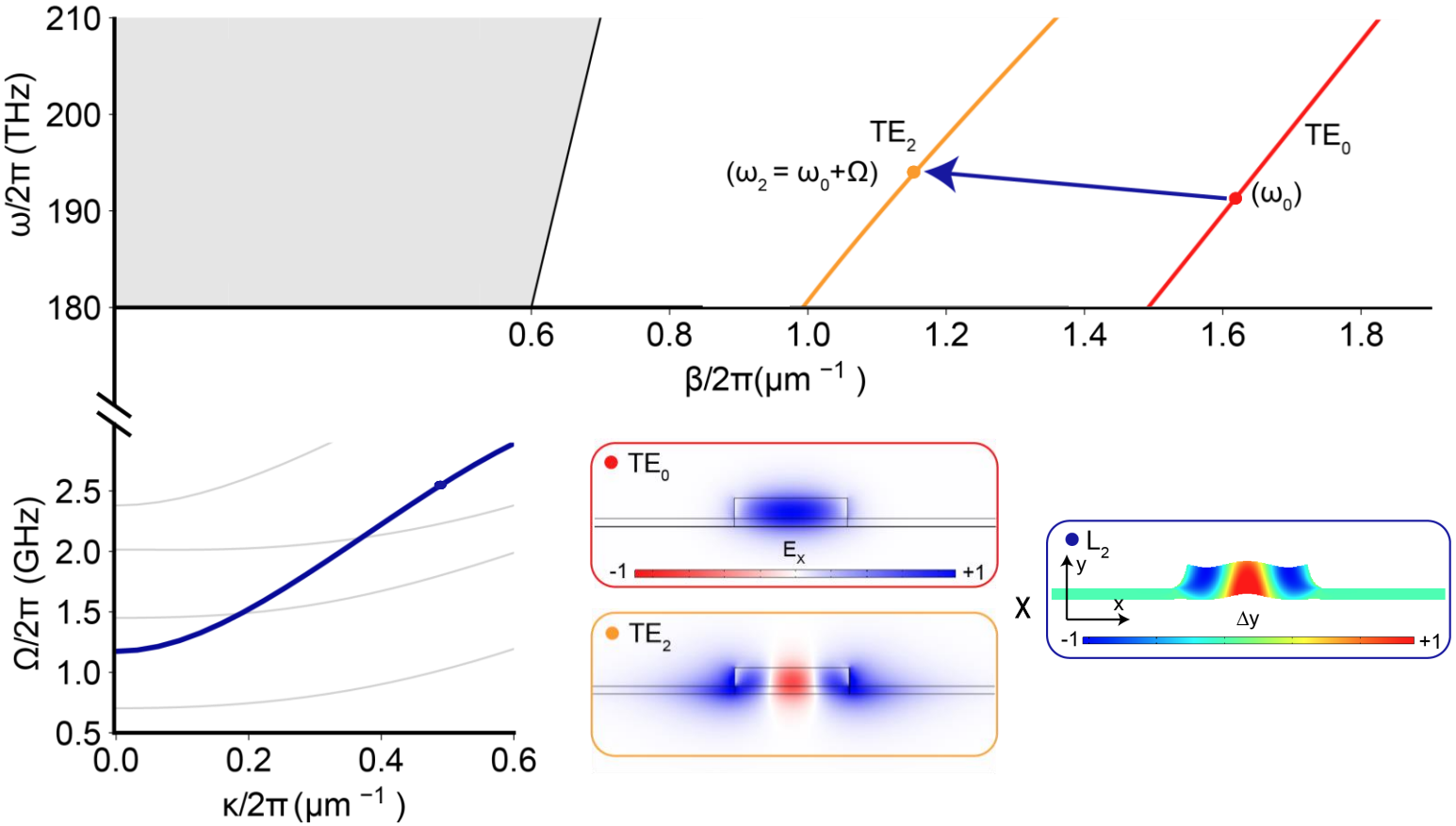

I.-T. Chen et al, Nat. Commun. 14, 7594 (2023).

Phononic modes characterization: reflection coefficient

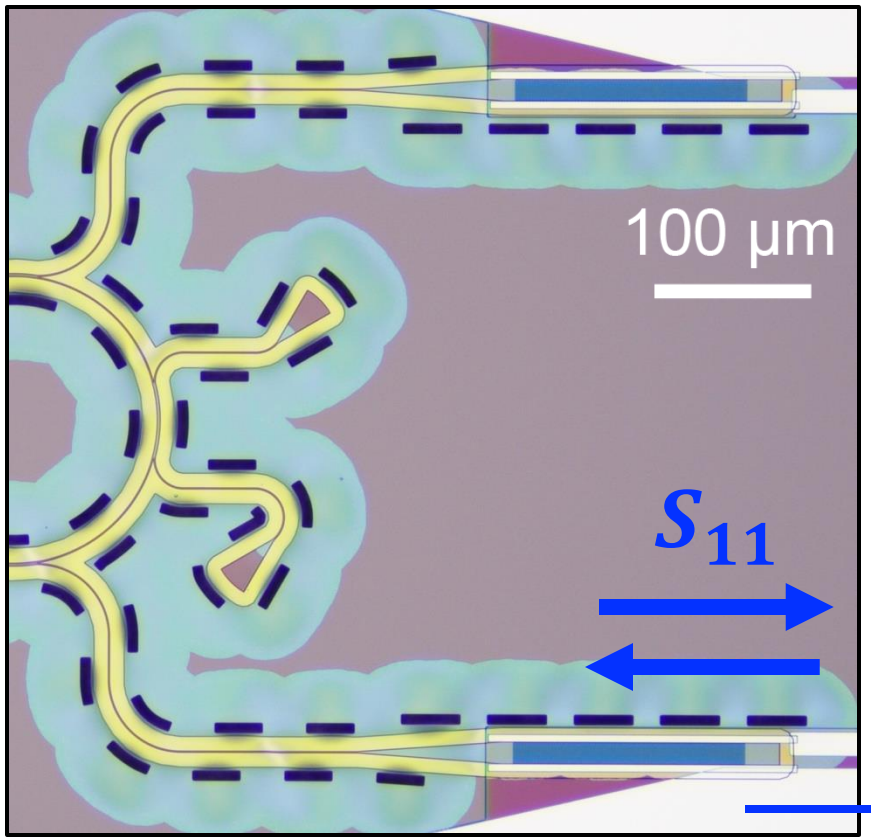

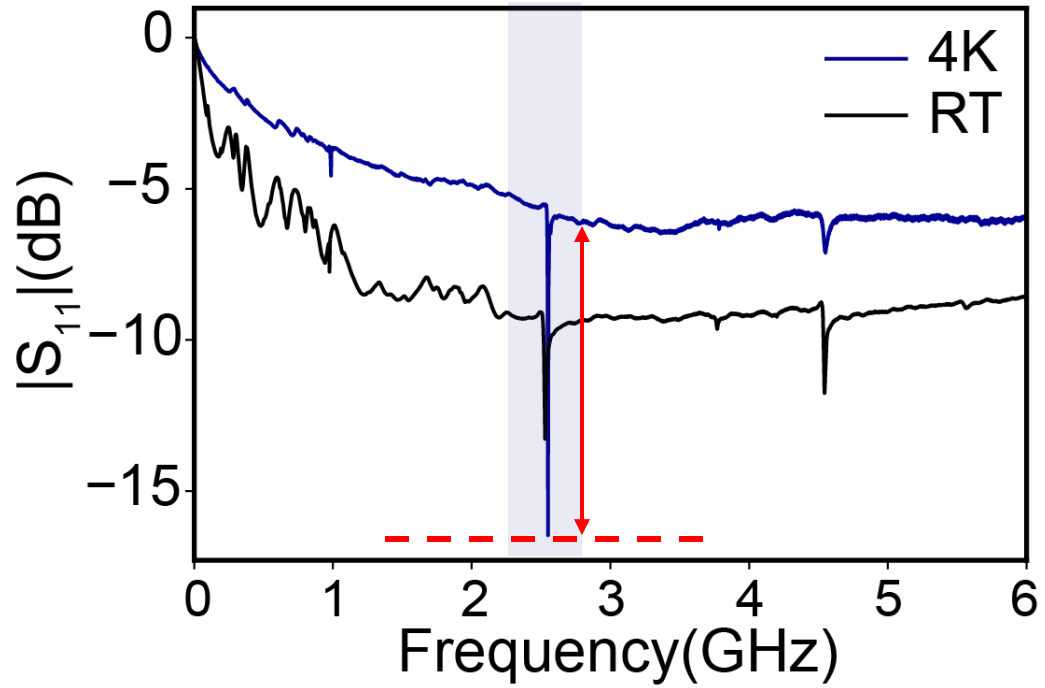

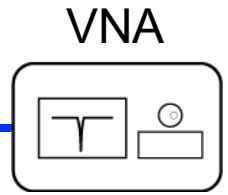

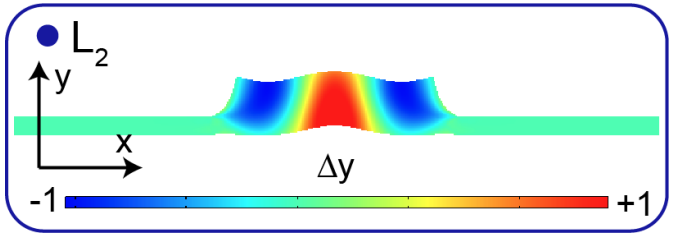

Microwave to phononic mode efficiency $\eta_{em} > 90\%$ at 4K by modified-BVD model

I.-T. Chen et al, Nat. Commun. 14, 7594 (2023).

Phononic modes characterization: transmission coefficient

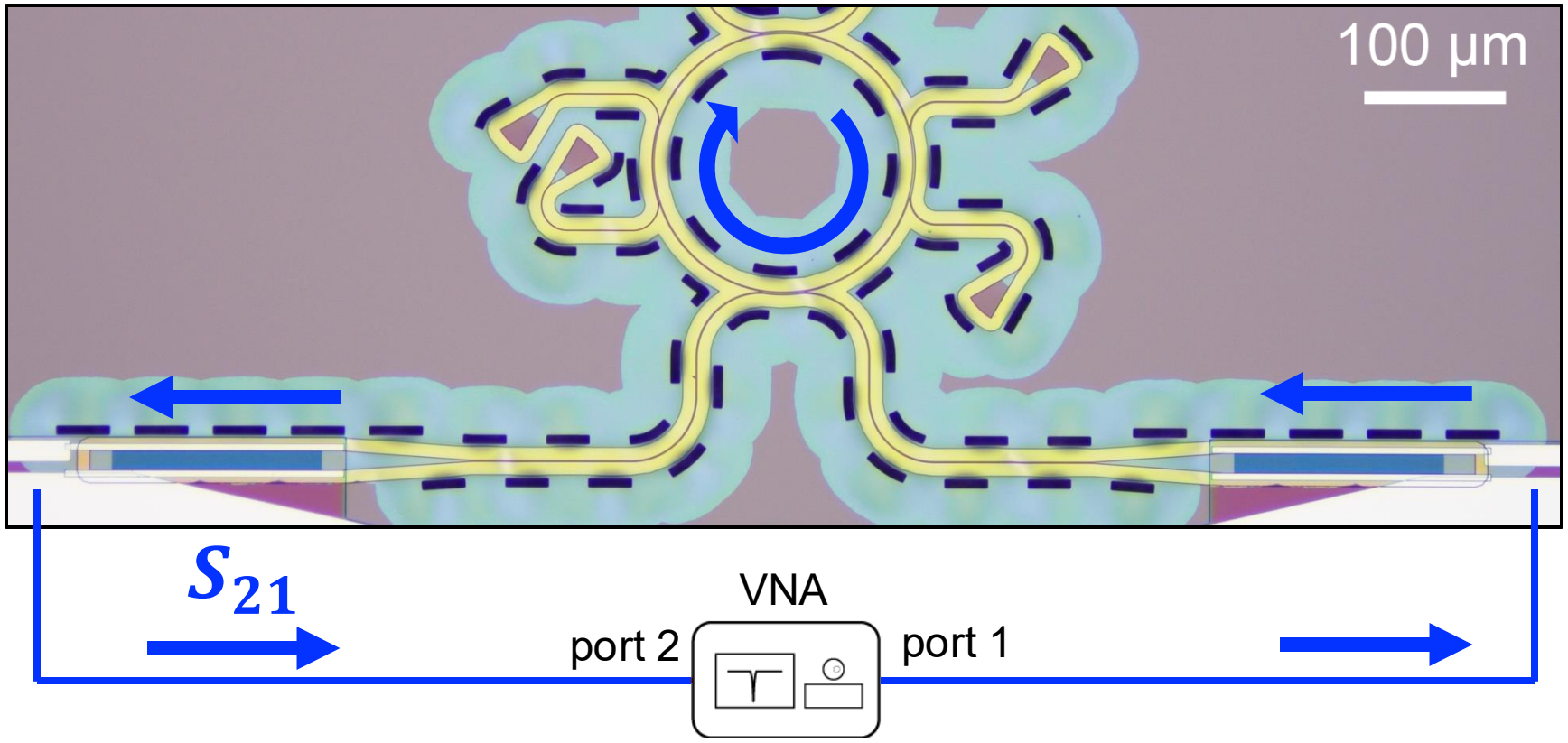

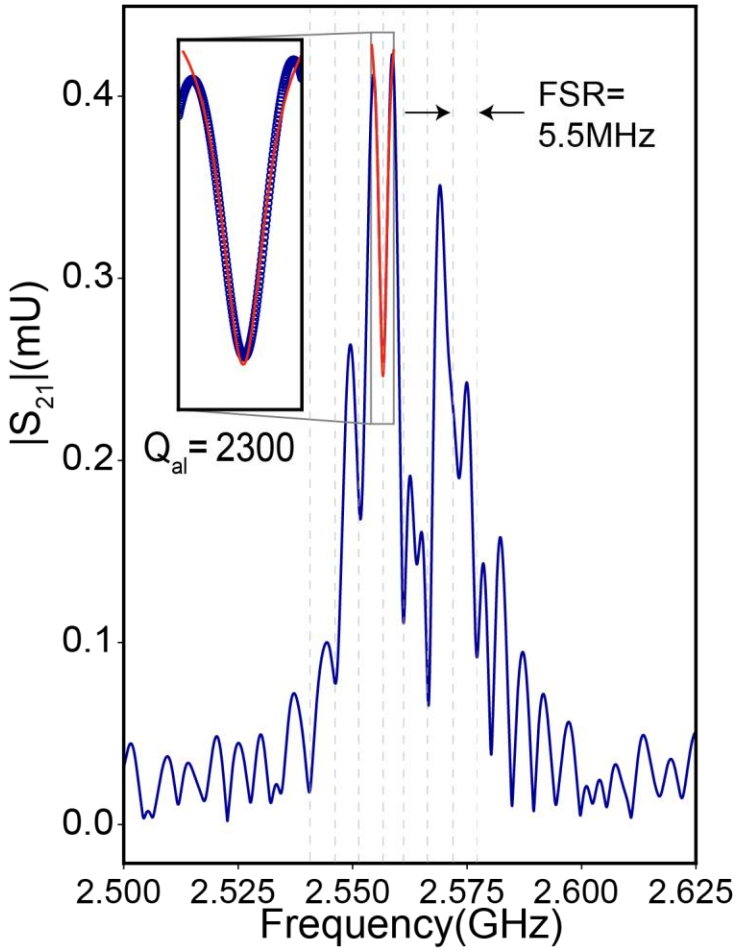

Multi-phononic resonances circulating in the OMR.
Loaded quality factor: $Q_a \sim 2300$

Photonic characterizations

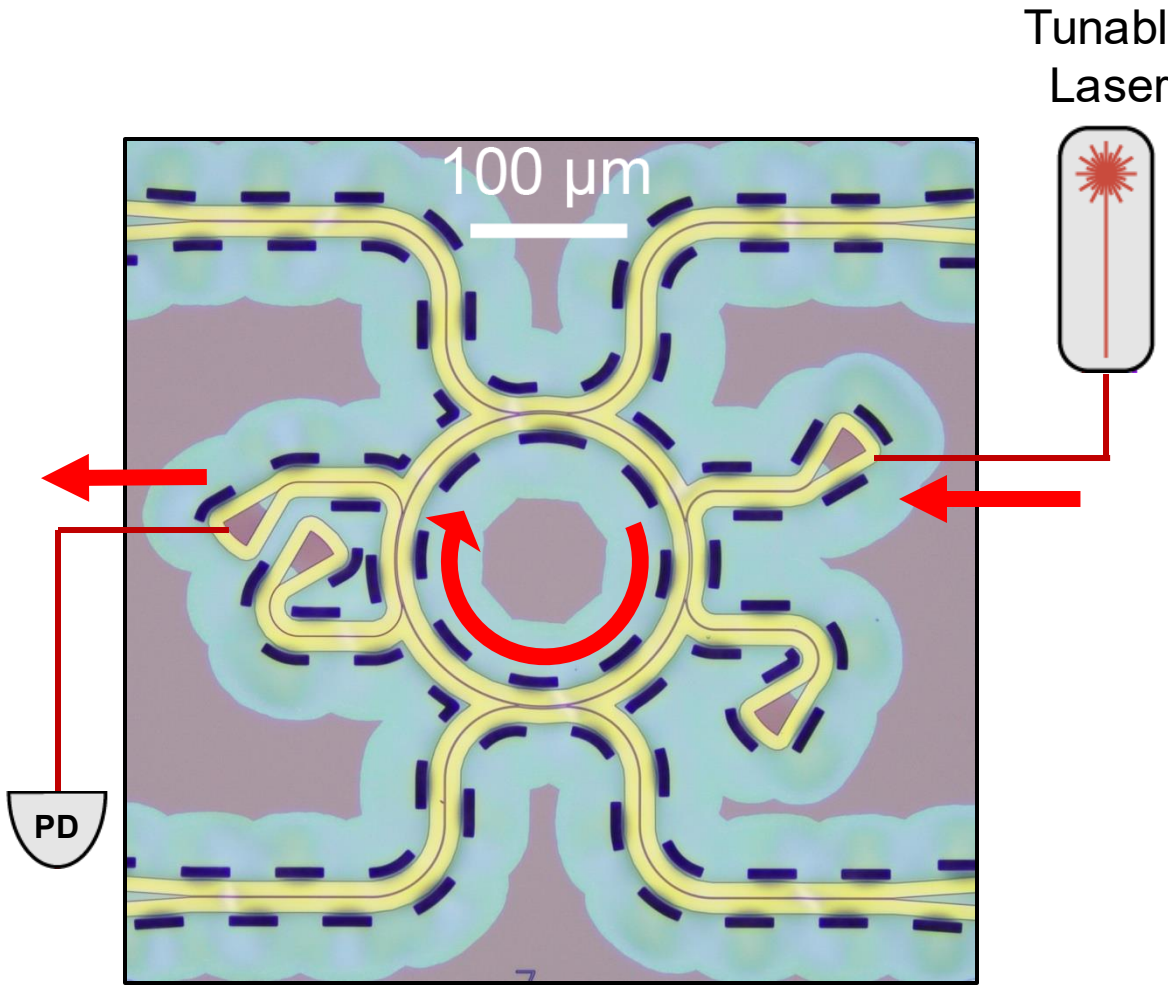

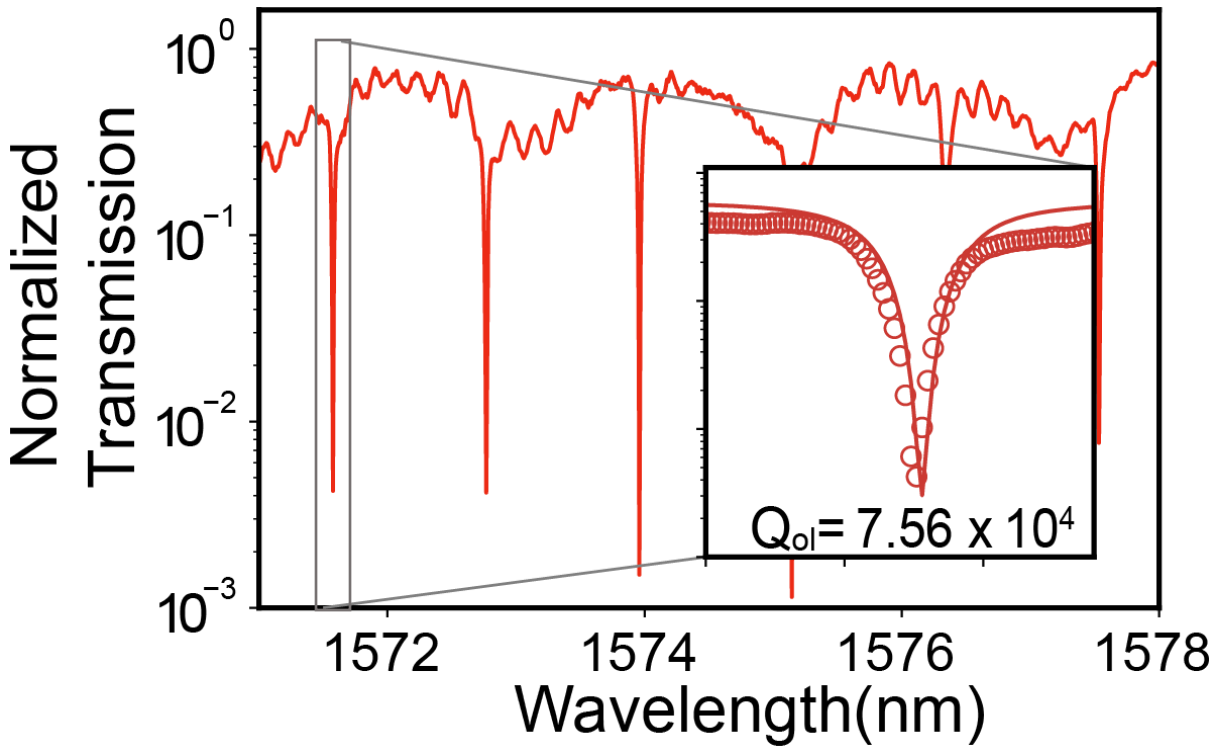

Loaded optical quality factor: $Q_o \sim 75{,}000$

I.-T. Chen et al, Nat. Commun. 14, 7594 (2023).

Device characterization: Time-reversal symmetry

Phase-matching condition:

$$\vec{\beta}_0 - \vec{q} + \vec{\beta}_1 = 0$$

(+): clock-wise

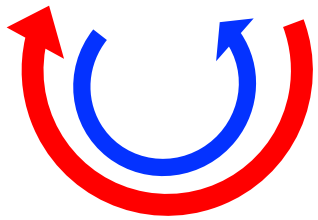

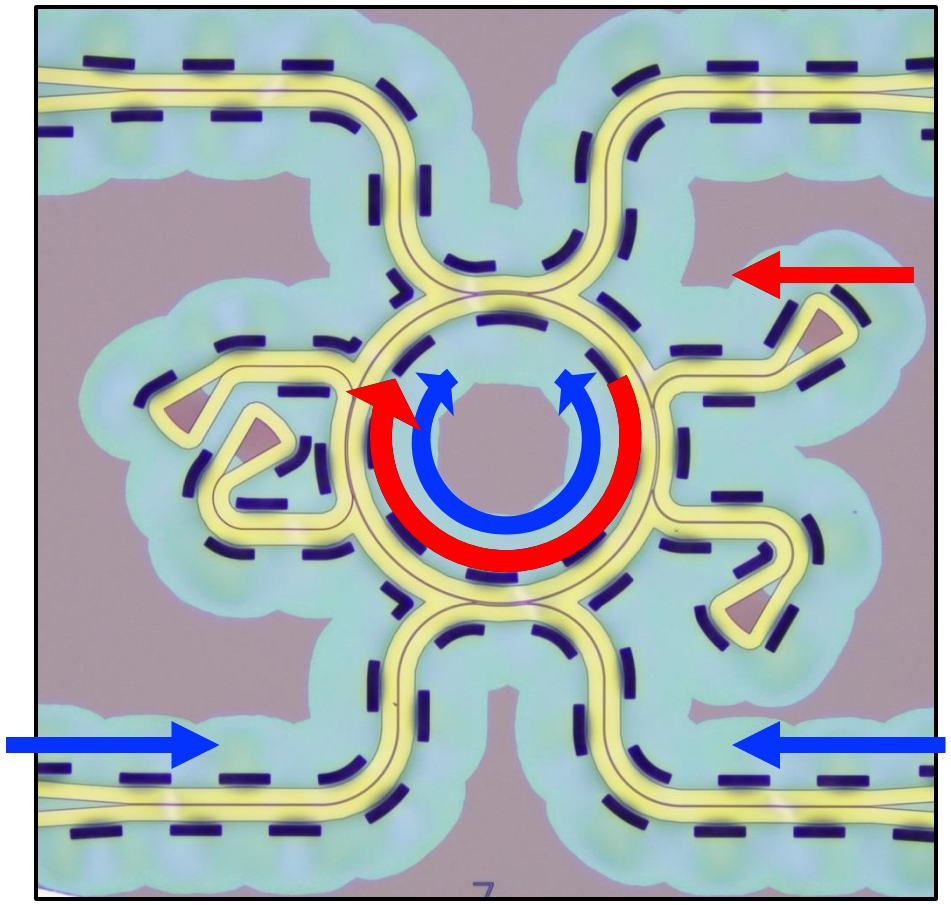

Output intensity received by an optical spectrum analyzer (OSA)
(fixed optical drive)

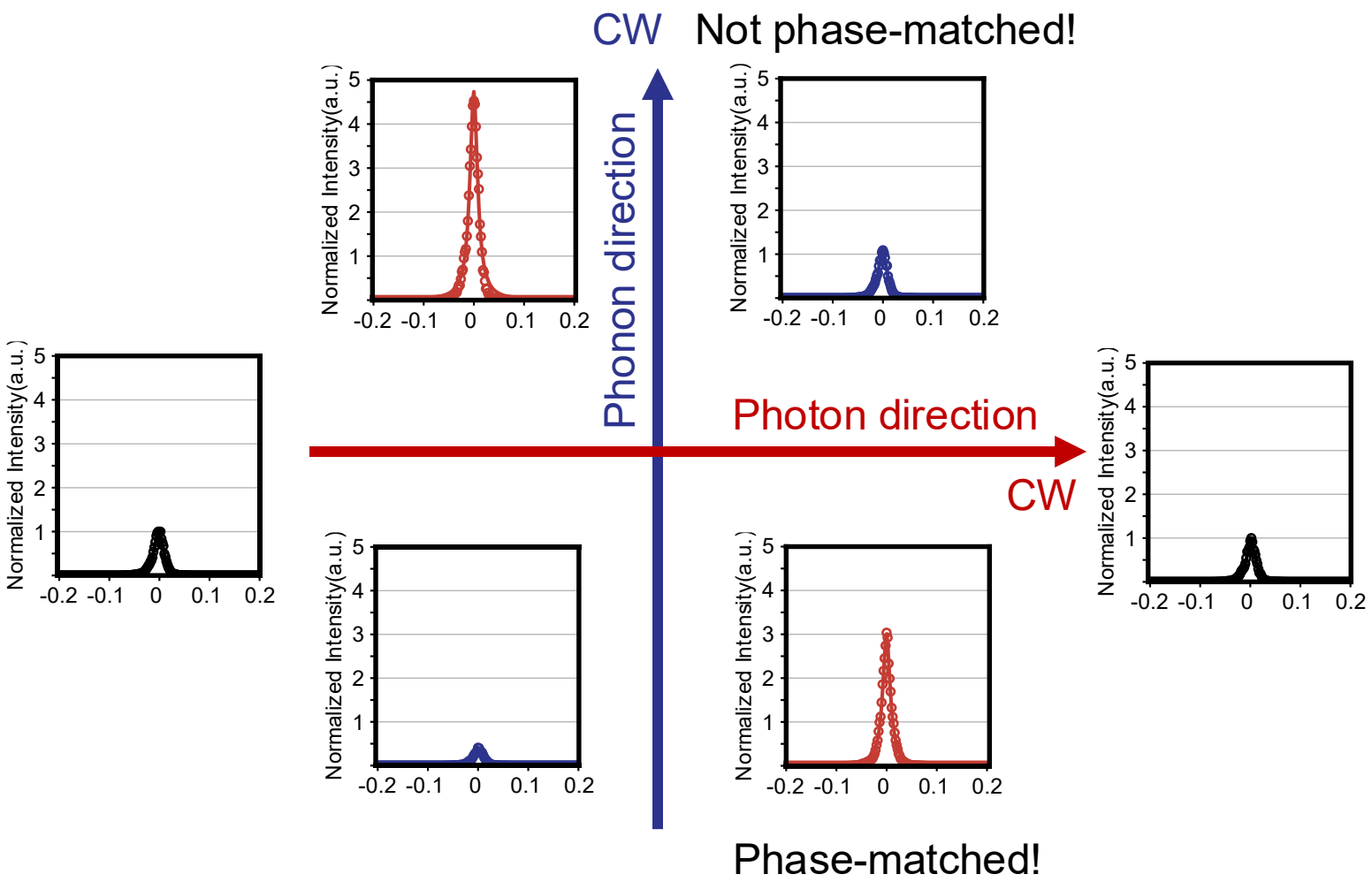

This indicates optomechanical coupling in OMIC

I.-T. Chen et al, Nat. Commun. 14, 7594 (2023)

Frequency resolved optical spectrum

Optical heterodyne measurements

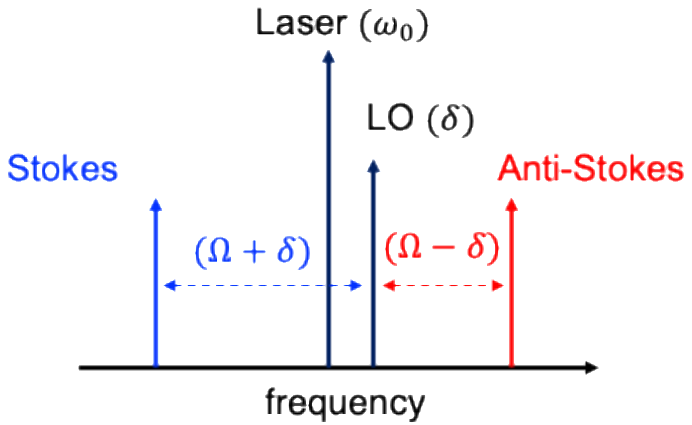

Beating signal in the optical spectrum

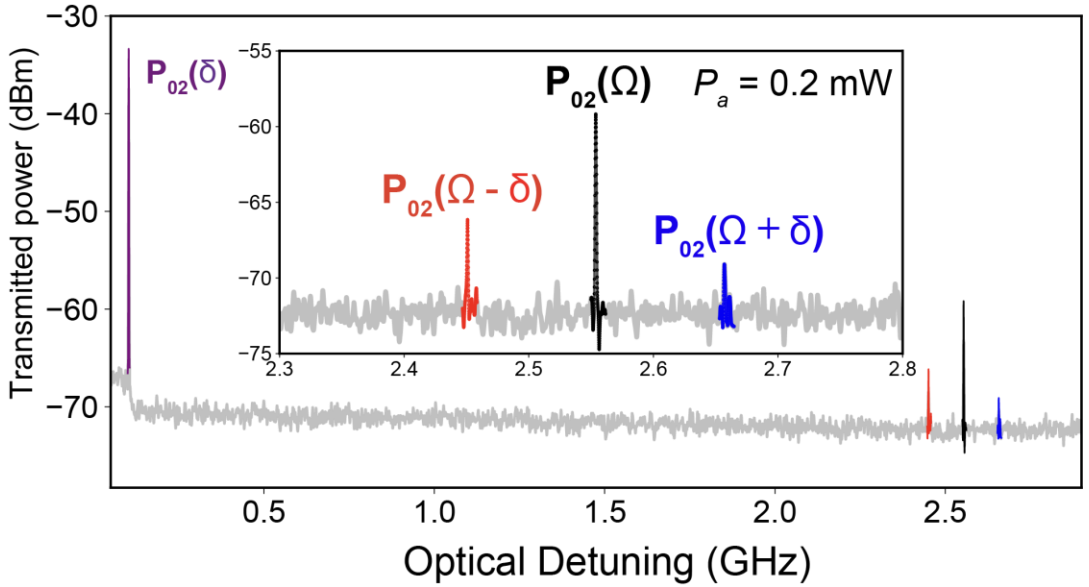

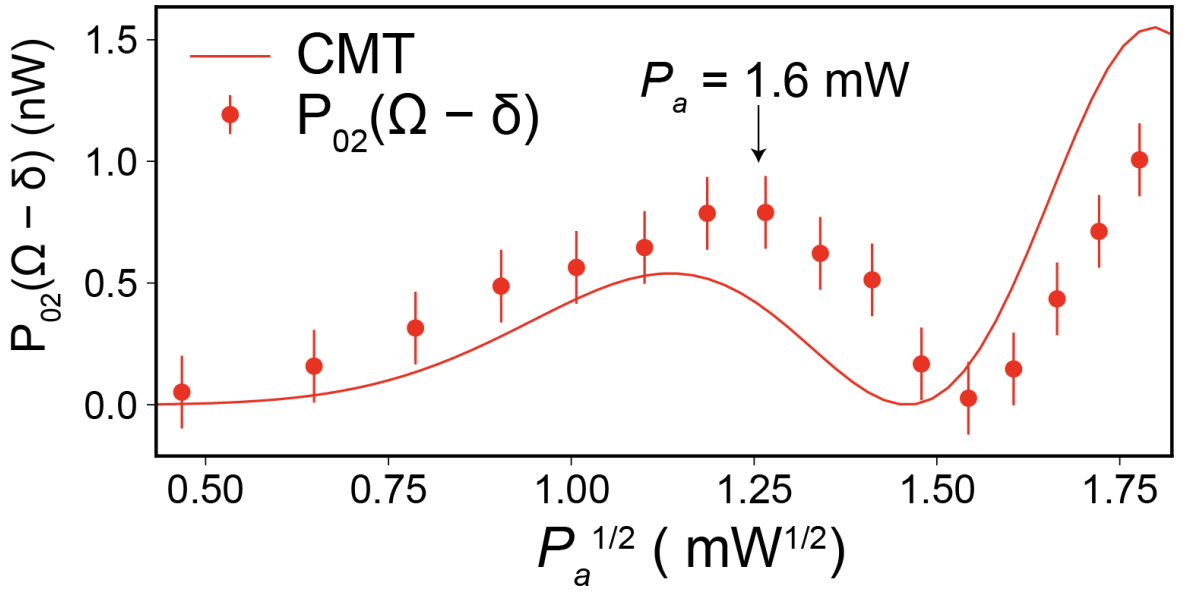

Coupled mode theory fitting (CMT):

$$A_2(z) = A_0(0)[-iG\frac{\sin(sz)}{s}]e^{i\Delta\beta z/2}$$

Oscillatory features: traveling wave cavity + multi-mode

microwave → phonons (Lamb mode) → optical (TE_2)

I.-T. Chen et al, Nat. Commun. 14, 7594 (2023)

Summary on the first OMIC

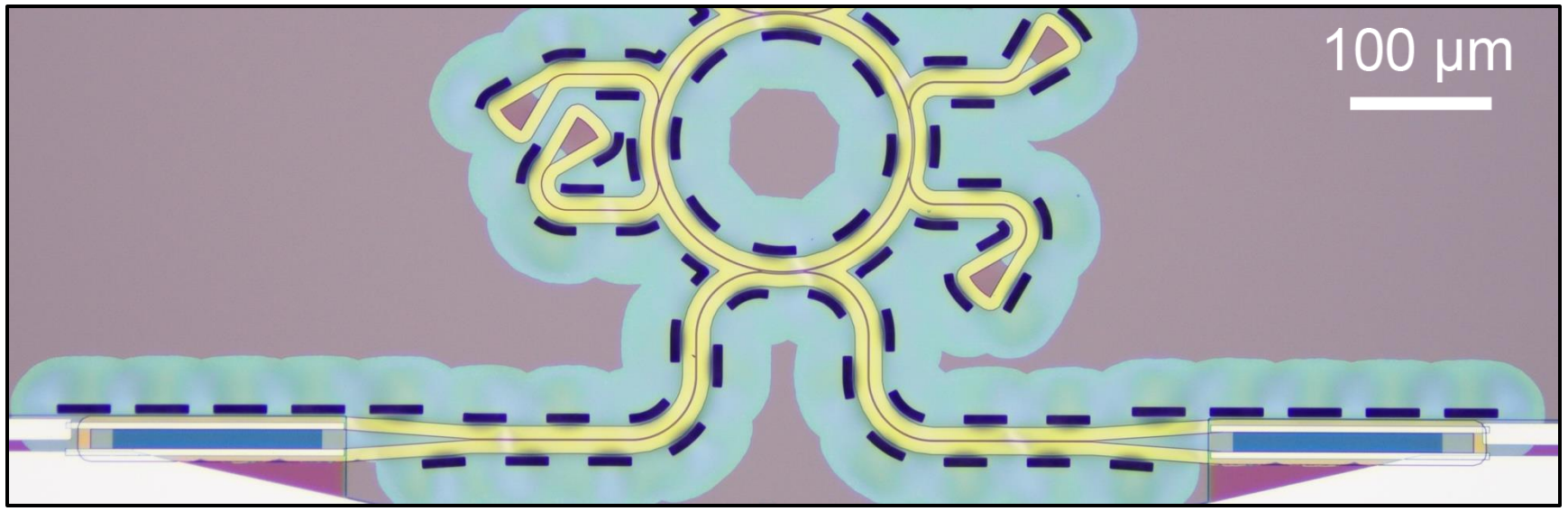

Feature:

- The first optomechanical integrated circuit (OMIC) and ring resonator (OMR)
- On a suspended BGaP thin film
- This is a hybrid platform: ZnO and BGaP

Problems:

- Suspended
  - Difficult to integrate with SC qubits
  - Optical induced heating limits the efficiency

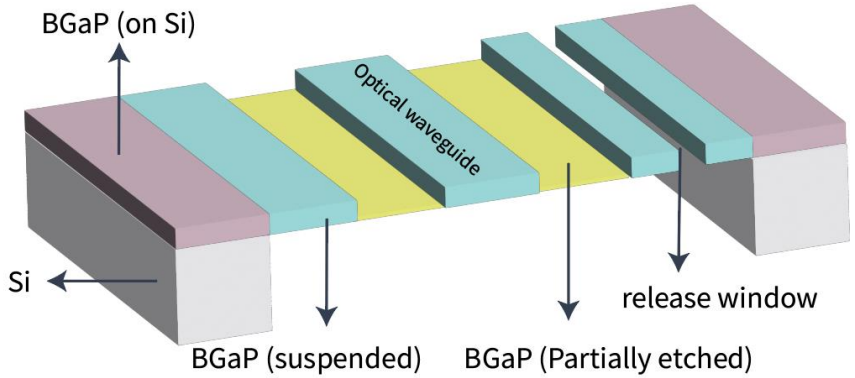

I.-T. Chen et al, Nat. Commun. 14, 7594 (2023)

Silicon-on-sapphire (SOS)

- Phononic waveguiding (v_{si}~$5000\ m/s$ vs. $v_{sapp.}$~$10{,}000\ m/s$)
- Photonic waveguiding (n_{si}~$3.4@1.55um$ vs. $n_{sapp.}$~$1.72@1.55um$)
- Compatible with silicon integrated photonics
- Compatible with many quantum platforms
  - Single photon source at 1.27 um: G-centers[1]
  - Millisecond coherence superconducting qubits[2]

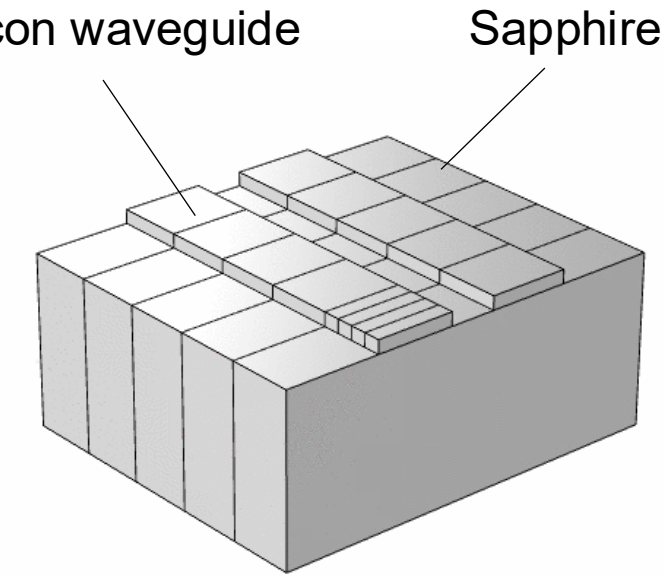

SOS phononic waveguiding

An ideal platform for optomechanical integrated circuits (OMIC)

[1] W. Redjem et al., *Nature Electronics*, *3*(12), 738-743. (2020)
[2] A. Somoroff et al., Phys. Rev. Lett. 130, 267001 (2023)

OMIC on silicon-on-sapphire (SOS)

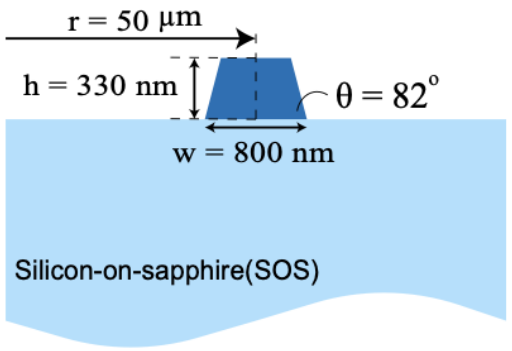

OMR

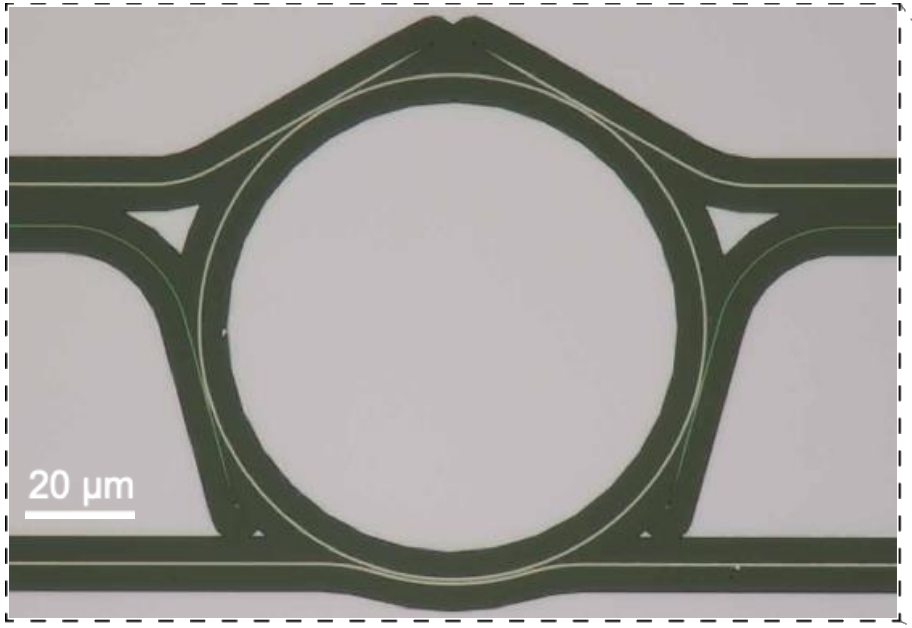

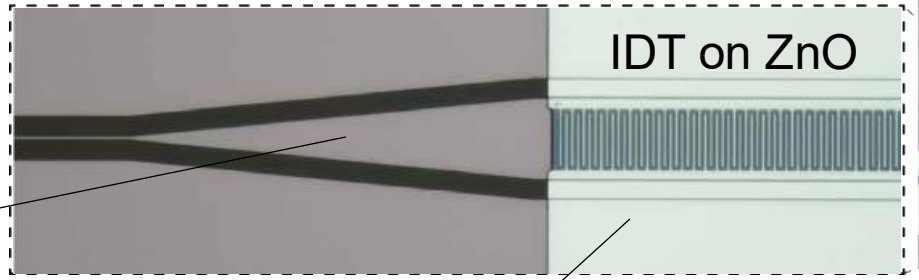

OMIC on SOS

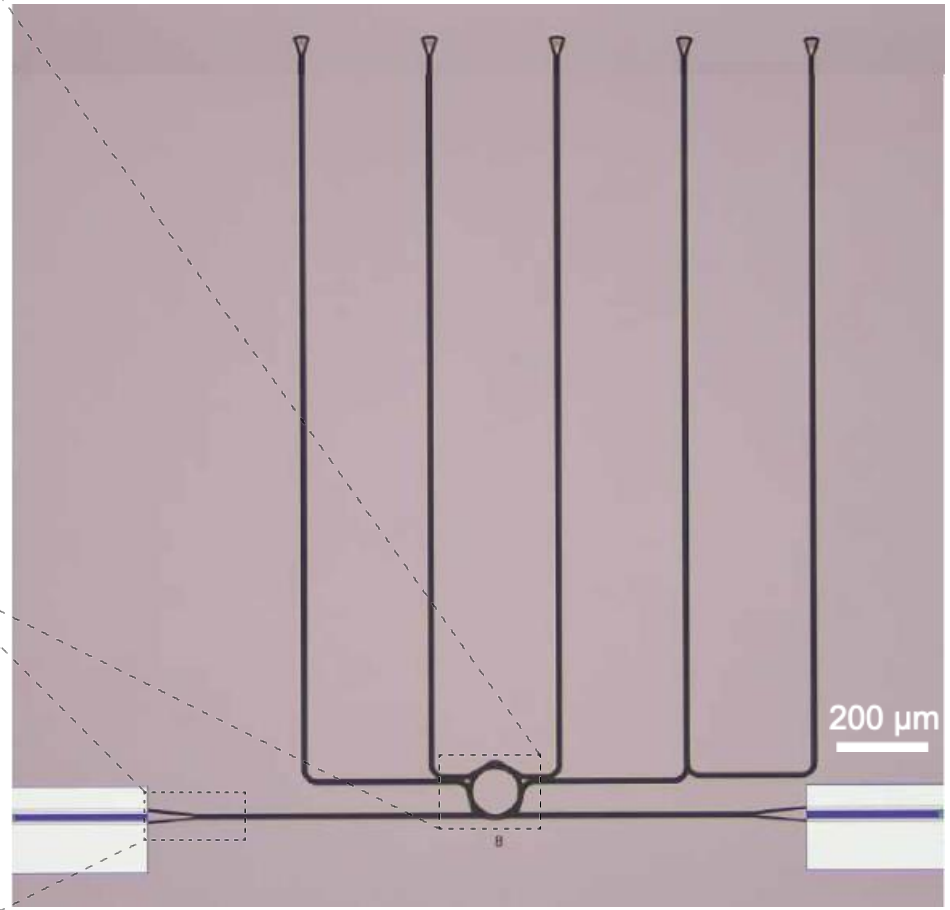

Phononic waveguide

Silicon is not piezoelectric, so a ZnO thin film is deposited to excite phononic mode.

Phase-matching condition

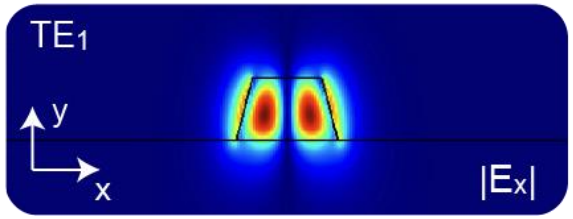

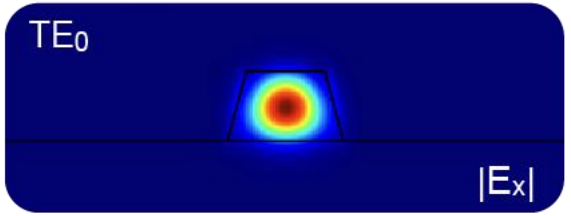

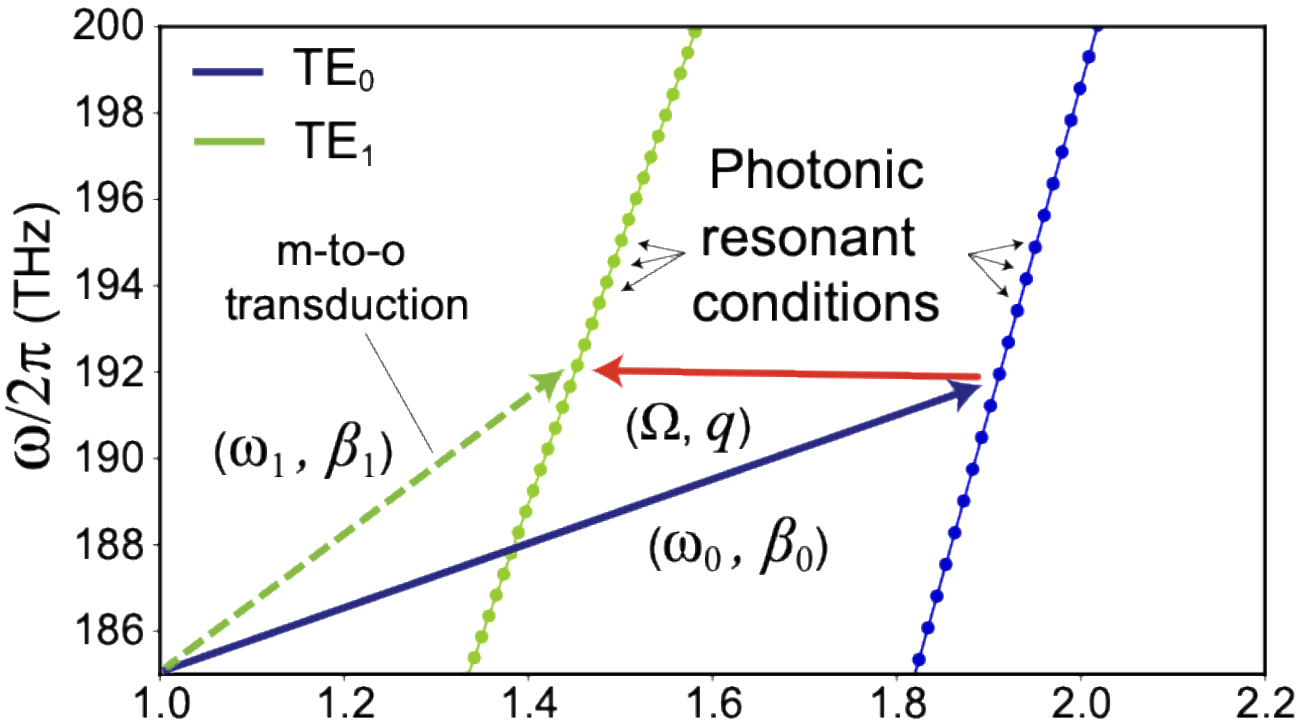

$$\hat{H}_{red} = \hbar G_{OMIC}(\hat{a}_1\hat{b}^\dagger + \hat{a}_1^\dagger\hat{b})$$

I. -T. Chen et al., submitted (2025)

Phononic waveguide resonances

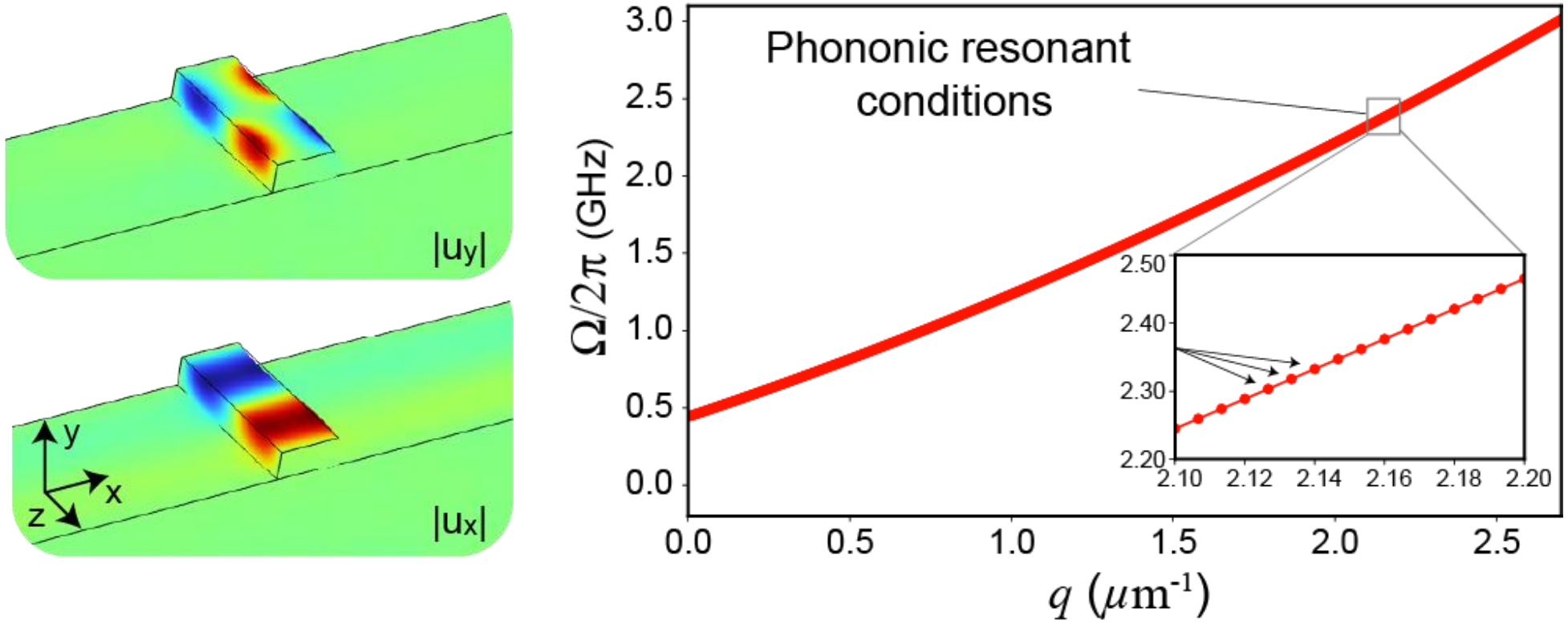

- First-order Love mode (L_0)
- Dispersion curve of the phononic modes in OMR, dots are resonances

Photonic resonance characterization

- Two pairs of waveguides (different widths) are used to selectively drive the photonic modes TE_0 and TE_1

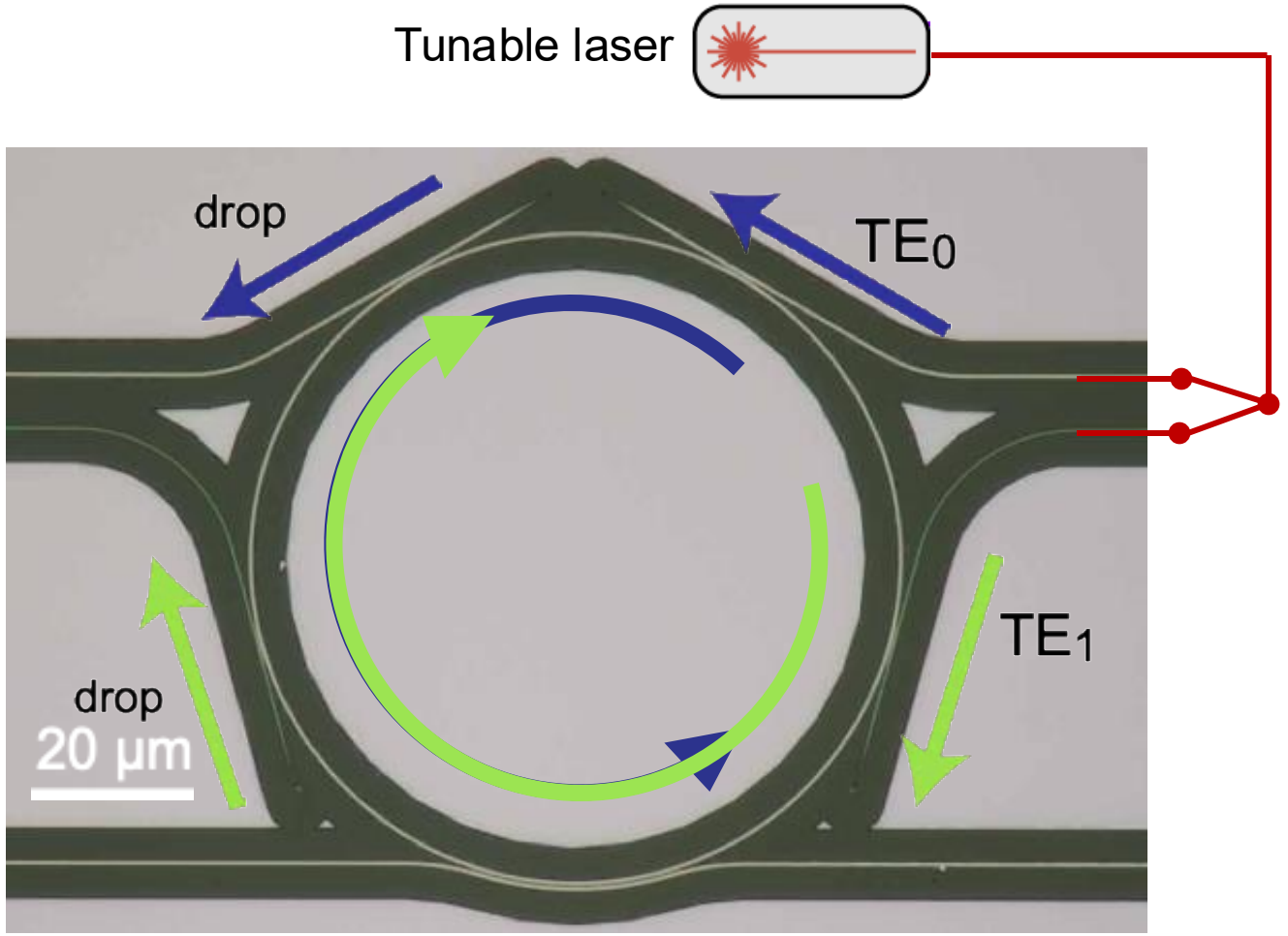

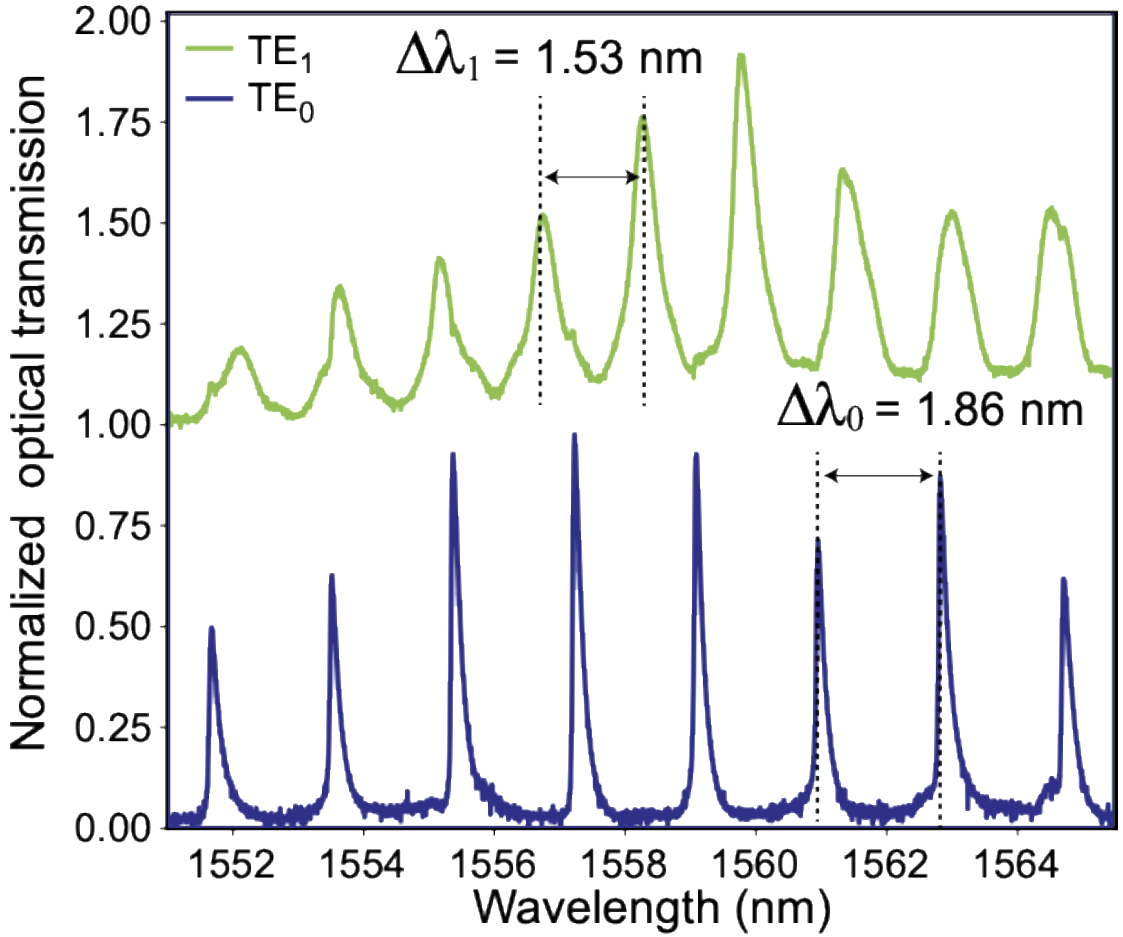

- Intrinsic quality factor $Q_0 = 100K, Q_1 = 8K$

I. -T. Chen et al., submitted (2025)

Photonic resonance characterization

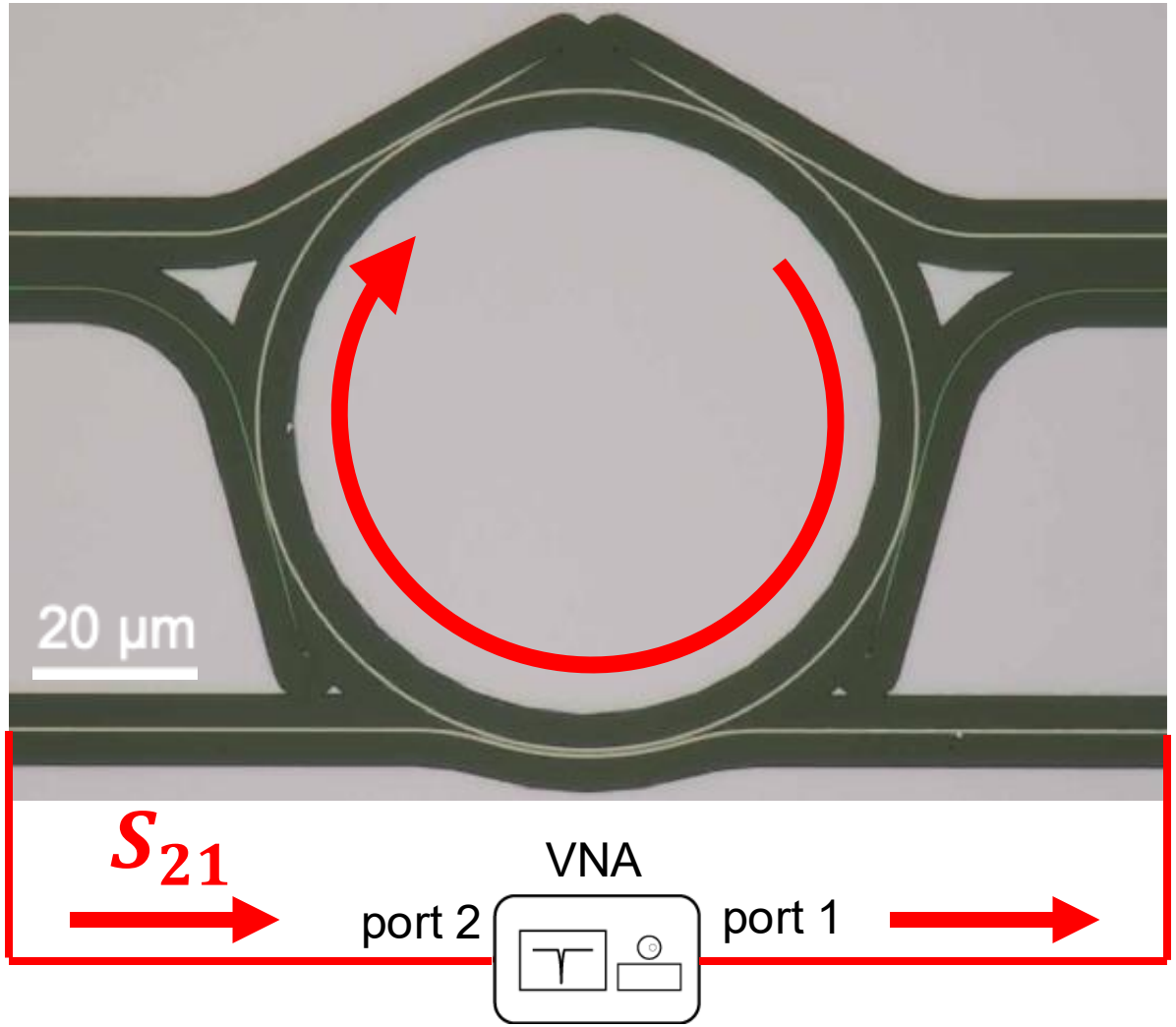

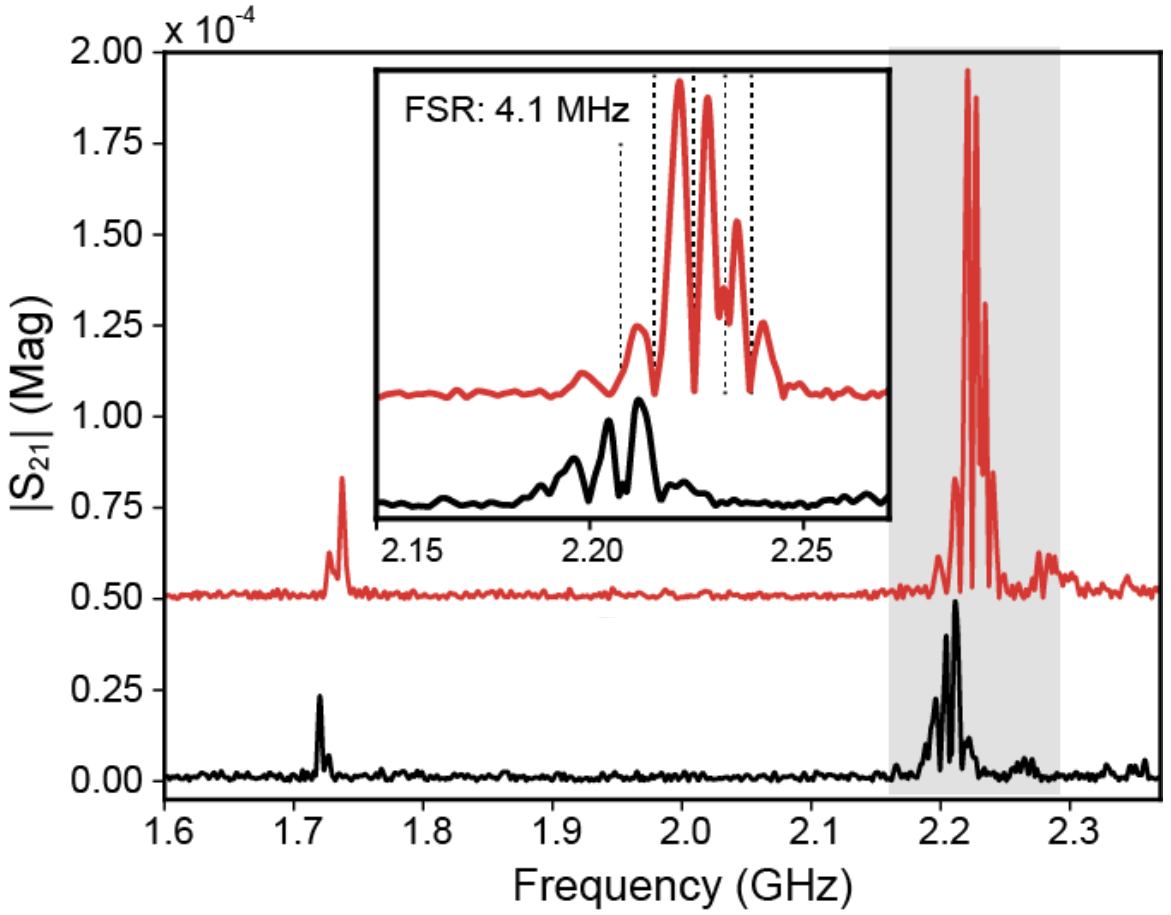

- Microwave transmission coefficient is used to measure the resonance of the phononic Love mode.
- Intrinsic quality factor $Q_L = 3K$ at 4K temperature

I. -T. Chen et al., submitted (2025)

Multi-resonances measurement setup

Driving TE_0 resonance and a sweeping microwave signal

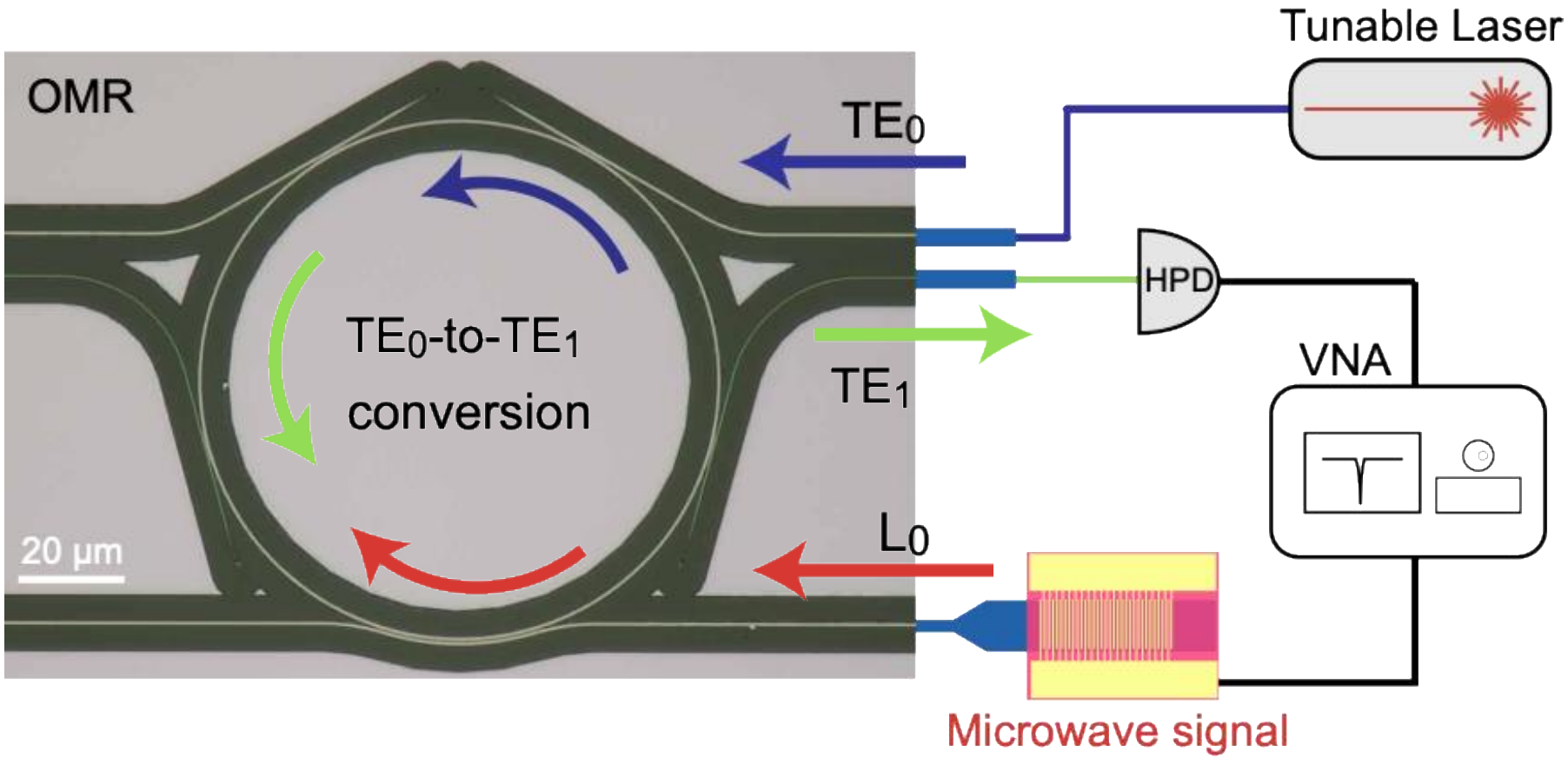

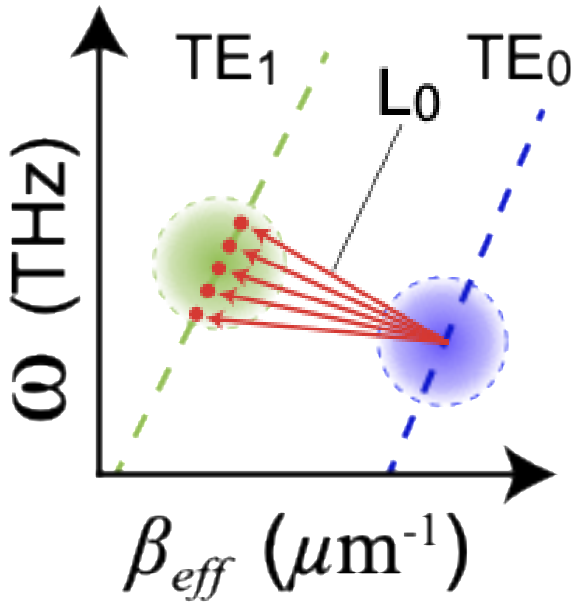

I. -T. Chen et al., submitted (2025)

Triple resonant microwave-to-optical transduction

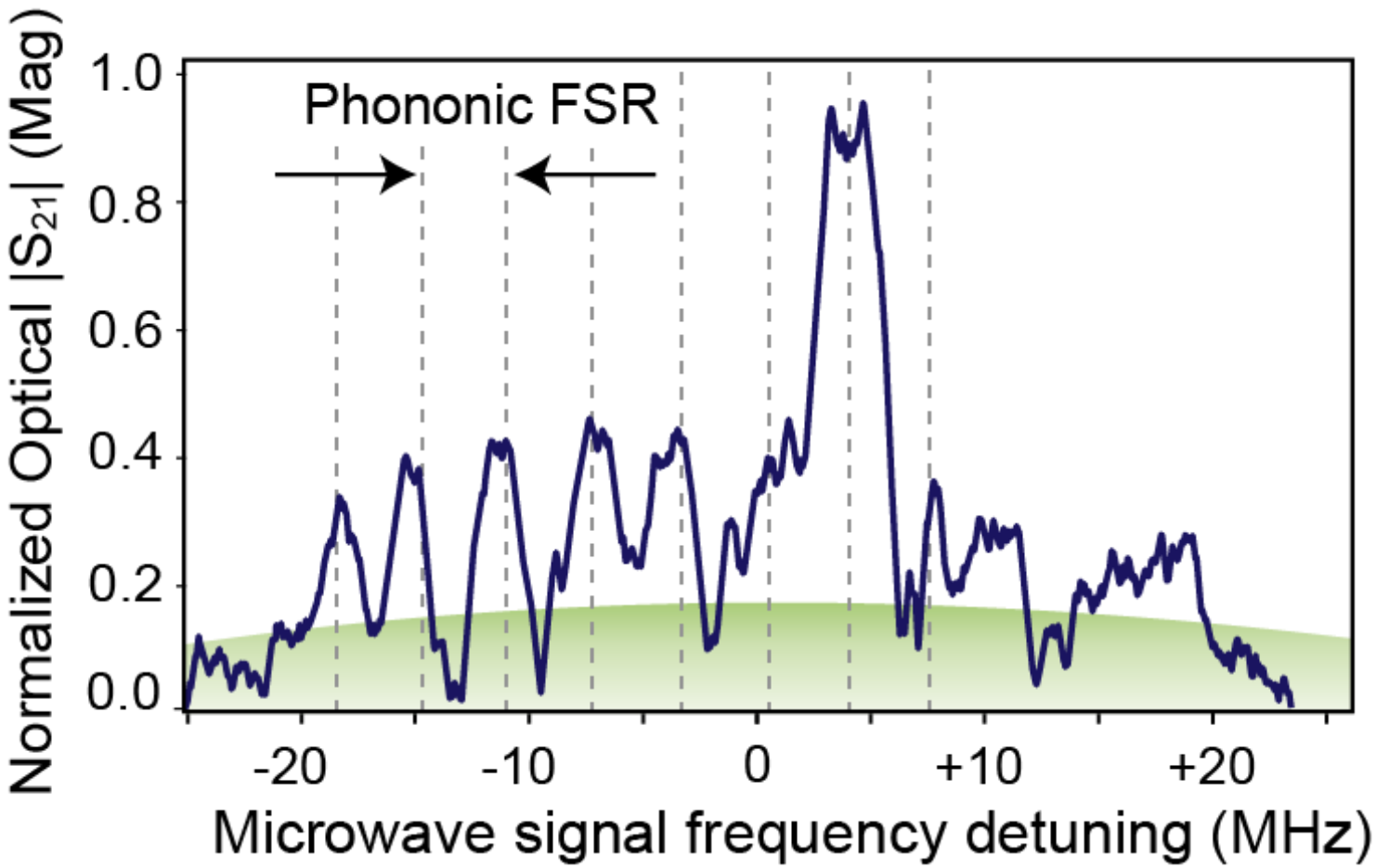

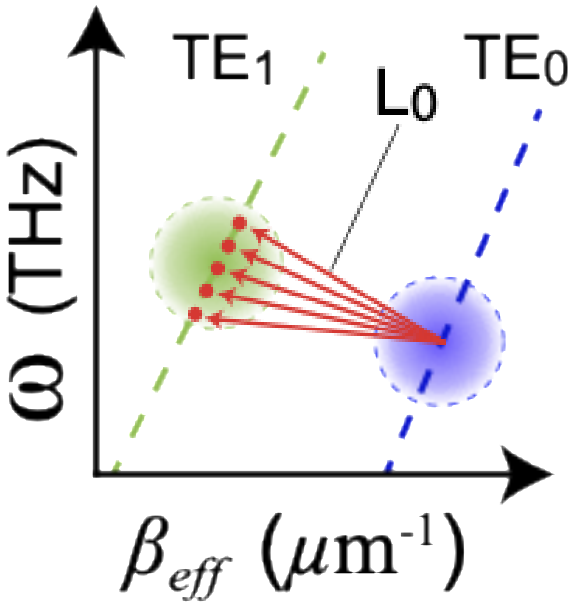

$$FSR = \frac{v_g}{L}\,(\mathrm{Hz})$$

One TE_1 resonance envelopes multiple L_0 resonances, a triple resonant condition (TE_0, TE_1, L_0).

I. -T. Chen et al., submitted (2025)

Multi-optical channels (wavelength division)

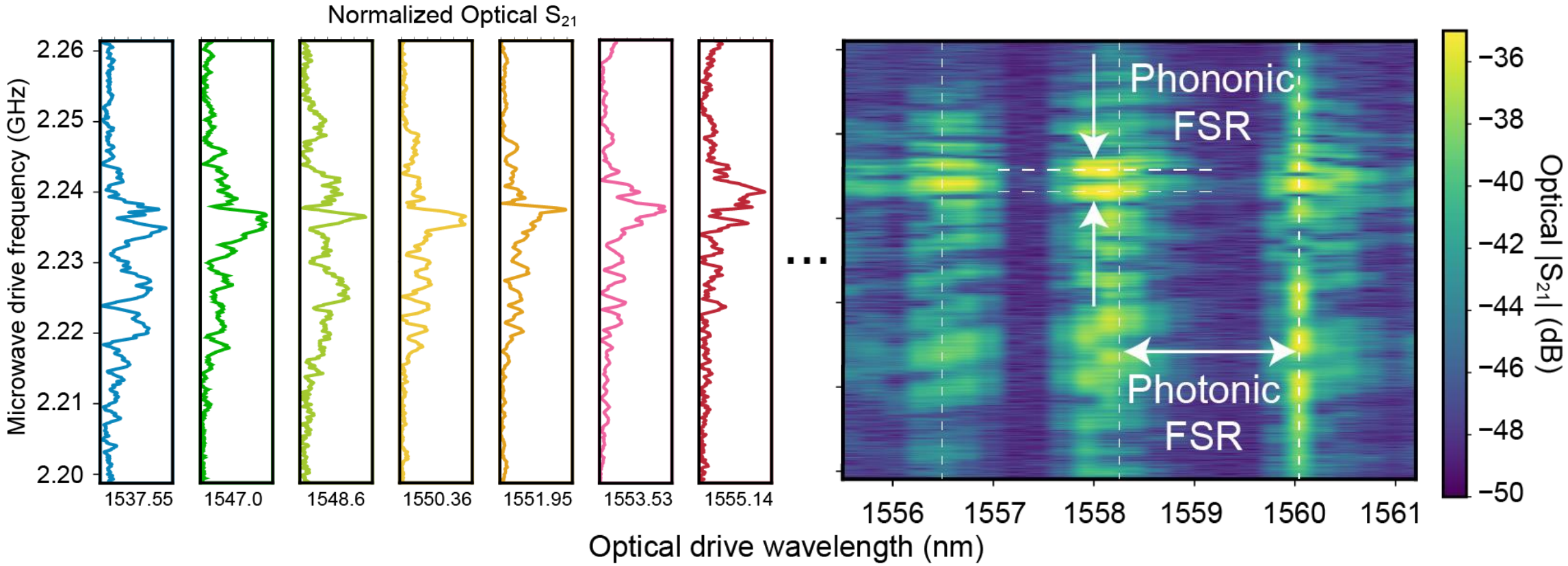

OMIC's microwave-to-optical transduction supports multiple channel/wavelengths

I. -T. Chen et al., submitted (2025)

Heterodyne measurements

Heterodyne measurement
Frequency resolved anti-Stokes (phonon absorption) and Stokes (phonon emission) signal

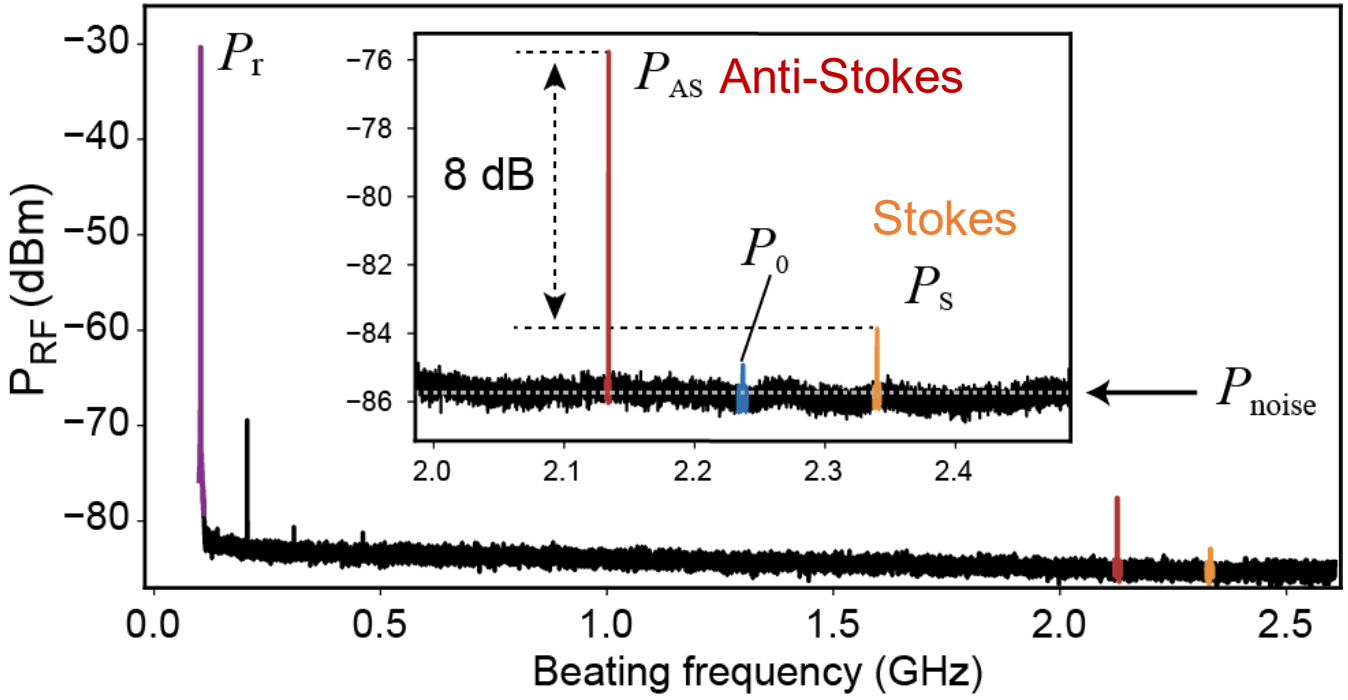

Single-frequency microwave signal

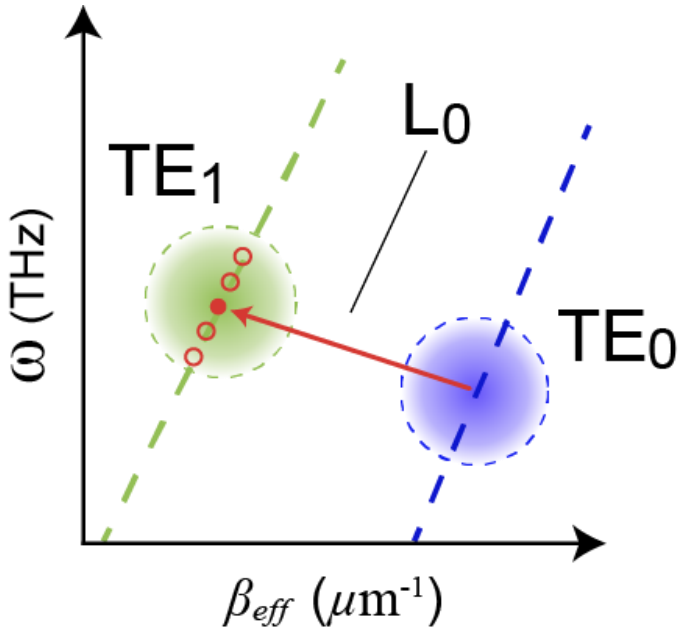

- Anti-Stokes signal dominates the intermodal microwave-to-optical conversion process
- Consistent with the phase-matching condition

I. -T. Chen et al., submitted (2025)

Heterodyne measurements with varying microwave power

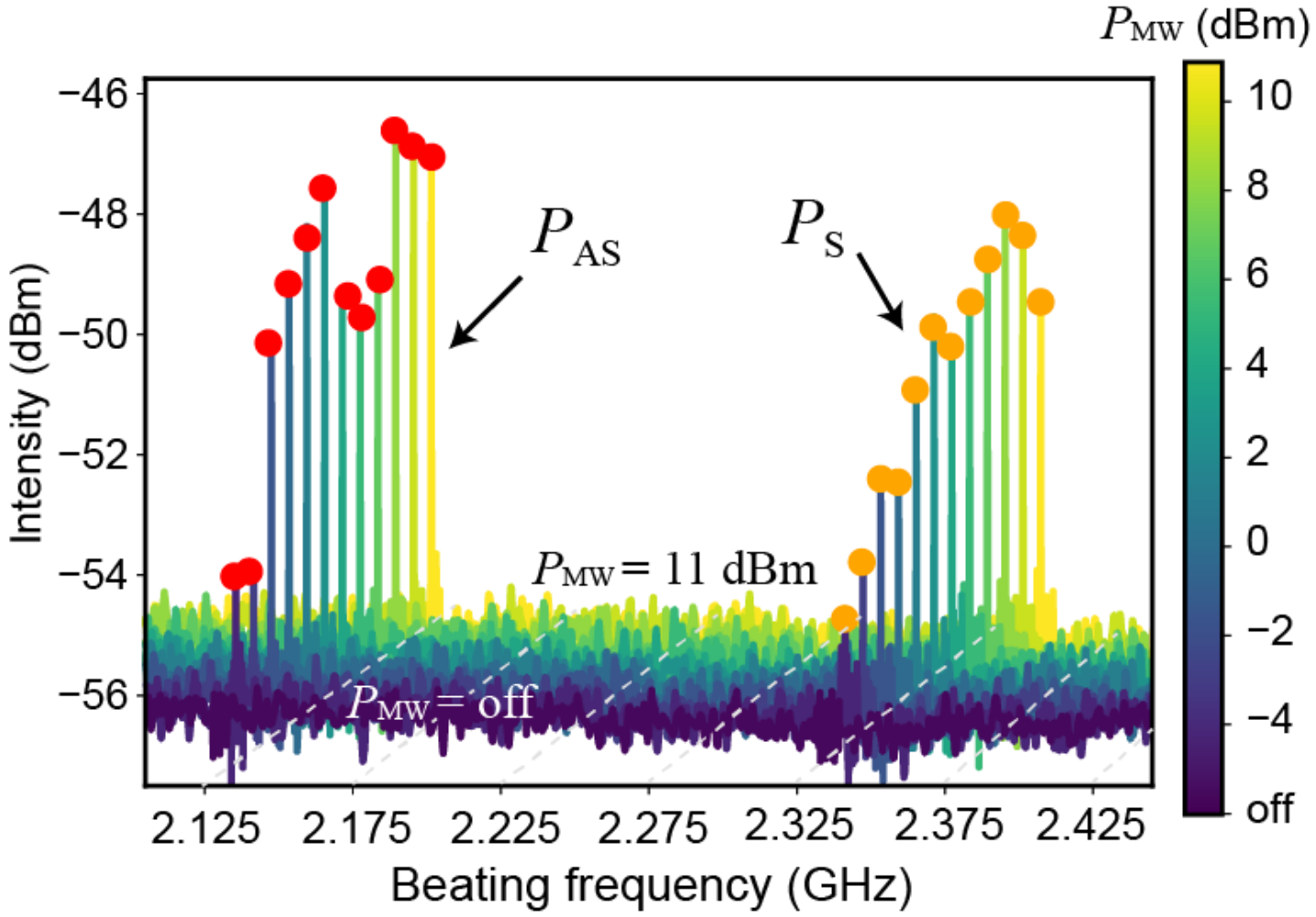

An oscillatory feature is observed when microwave power is increased

Microwave power dependent heterodyne signal

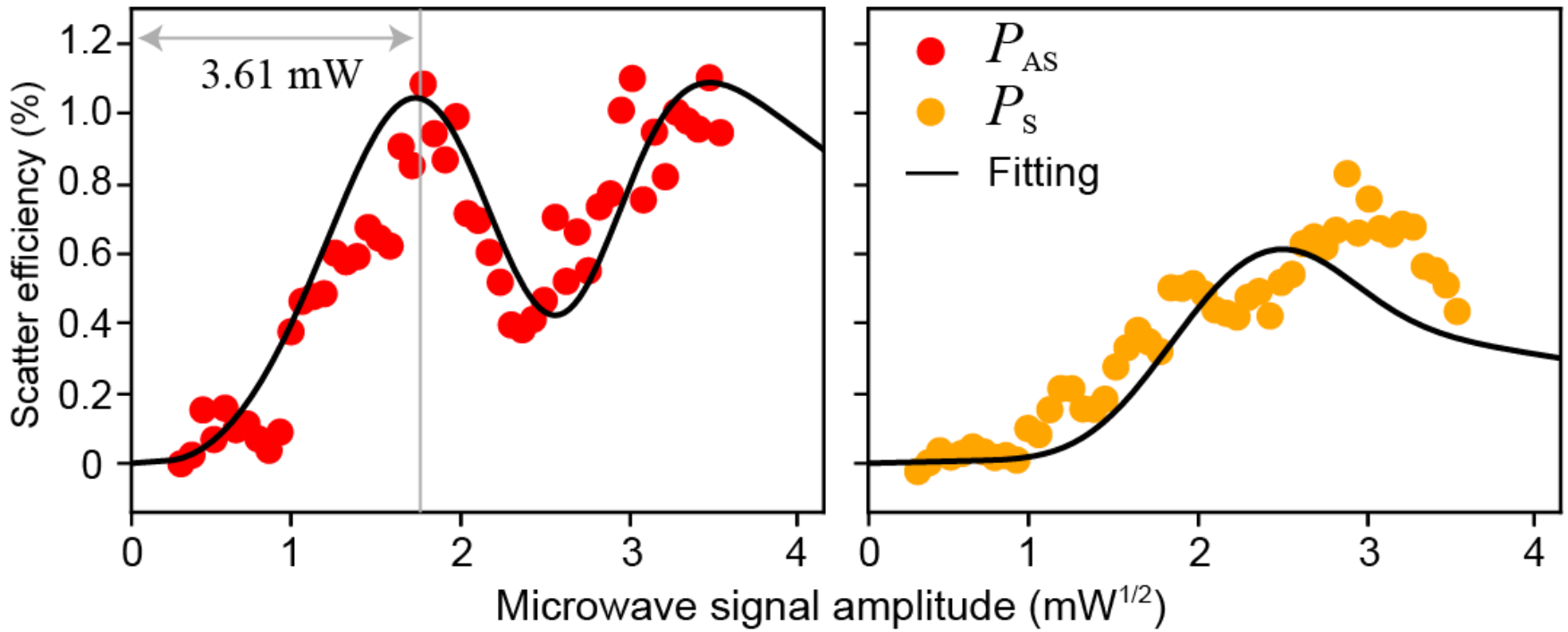

- The trace is fitted with OMIC input-output model to extract g_0
- The vacuum optomechanical coupling rate $g_0 \sim 350\,Hz$, with a theoretical limit: $g_0 = 15$ kHz
- TE_0-to-TE_1 efficiency saturates at 1.2%, which can be attributed to the imperfect photonic-phononic overlap

I. -T. Chen et al., submitted (2025)

Summary and future directions

Summary

- Developed the optomechanical integrated circuit (OMIC) theory for quantum transduction
- Realized and characterized OMIC and optomechanical ring resonator (OMR)
- Utilized a scalable silicon-on-sapphire (SOS) platform for microwave-to-optical transduction

Future directions

- Works with g_0 on the same order has demonstrated qubit readout[1][2]
- Quantum regime microwave-to-optical transduction
- Photon-phonon entanglement experiments
- Superconducting qubits optical read-out/control using OMIC/OMR

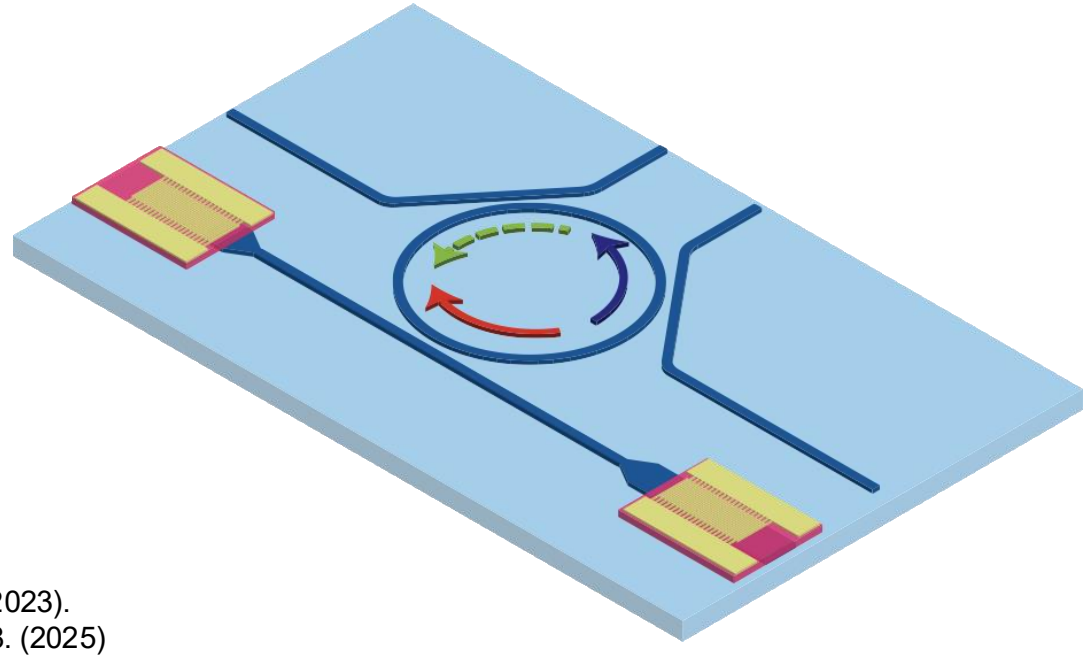

Transduction

$$\hat{H}_{red} = \hbar G_0(\hat{a}_1\hat{b}^\dagger + \hat{a}_1^\dagger\hat{b})$$

Entanglement

$$\hat{H}_{blue} = \hbar G_1(\hat{a}_0^\dagger\hat{b}^\dagger + \hat{a}_0\hat{b})$$

[1] Sahu, R. Science 380, 718–721 (2023).
[2] Warner, H. K., Nature Physics, 1-8. (2025)

Acknowledgements

Prof. Mo Li

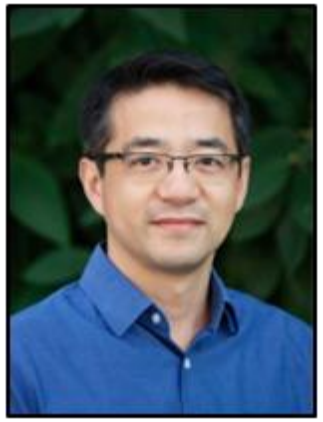

Prof. Kai-Mei Fu

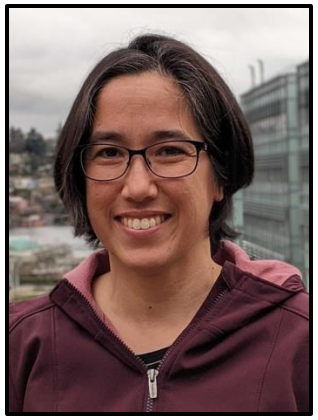

Laboratory of Photonic Systems (LPS) – Mo Li group

Prof. Arka Majumdar
Dr. Bingzhao Li
Dr. Seokhyeong Li
Dr. Srivatsa Chakravarth
Dr. Abhi Saxena
Nick Yama
Haoqin Deng
Qixuan Lin
Yue Yu
Adina Ripin
Shucheng Fang
Ameya Velankar
Mark Han

Fundings

DARPA
NSF
Washington Research FOUNDATION

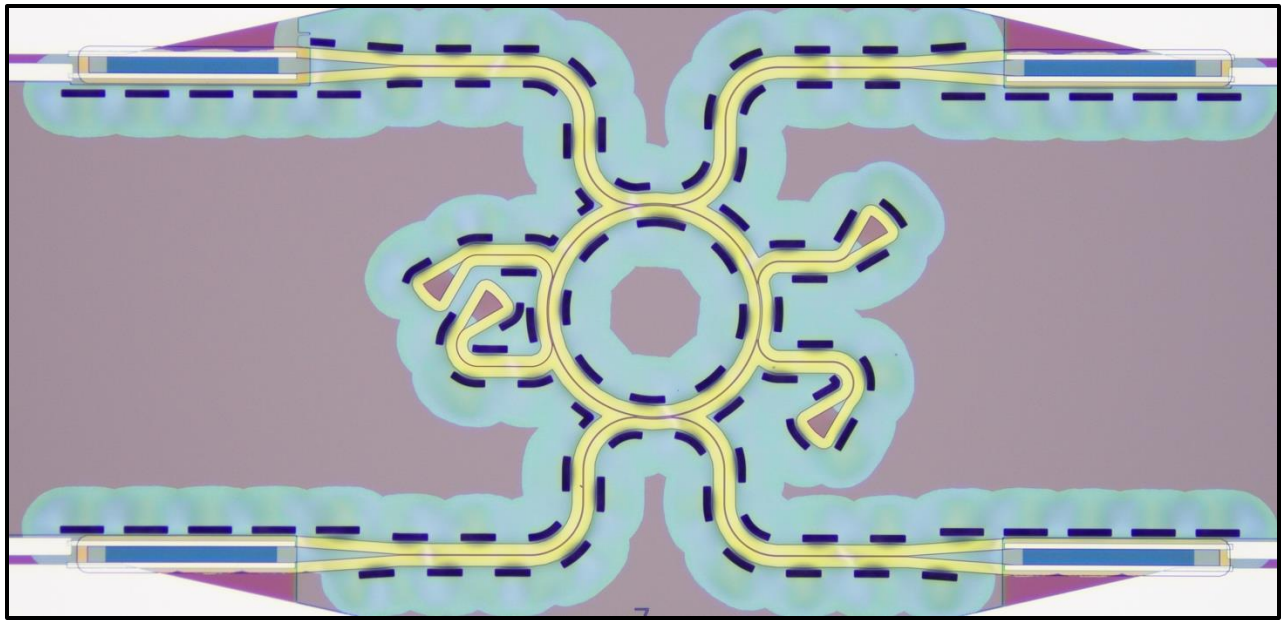

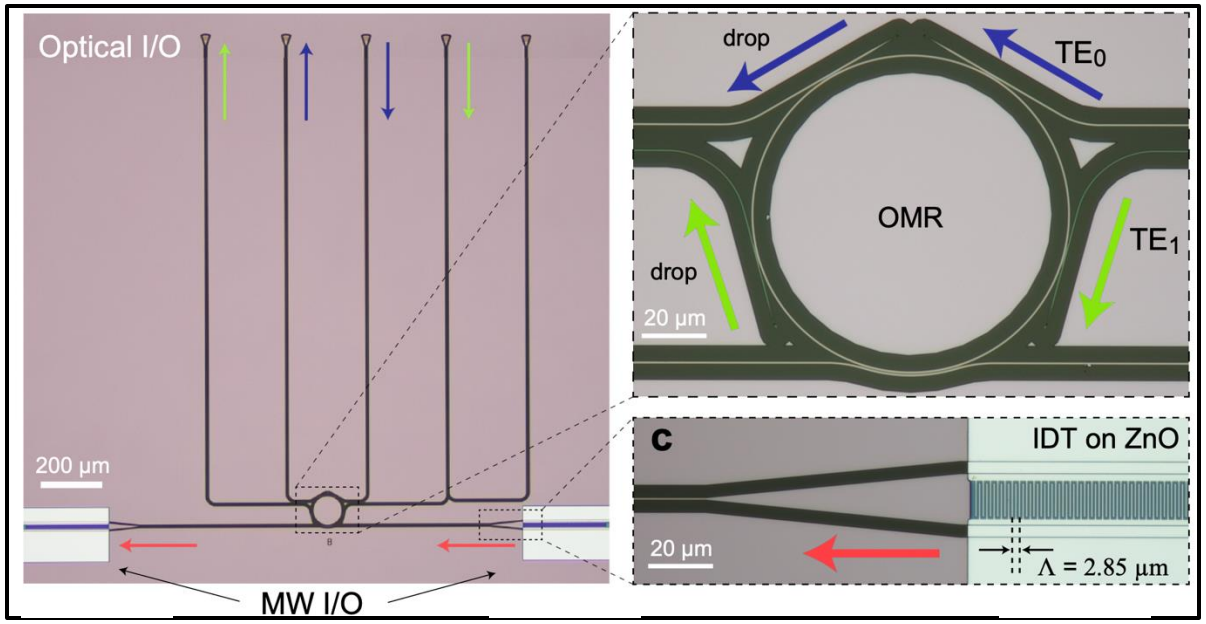

Supporting slides

Scalability of photonic links

Benefits of photonic links

1. Low loss (temperature independent)
2. Dense wavelength division multiplexing (DWDM)
3. Reduced passive heat load at mK

Passive heat-load						
Stage	Temperature	Cooling power (W)	Per co-axial cable	Number of cables	Per optical fiber	Number of fibers
4 K	$\sim 3K$	1.5	1 mW[1]		5.6 μW[2]	
MXC	$\sim 0.006K$	19×10^{-6}	~ 10 nW[3]	10^3	~ 5 pW[3]	$\mathbf{10^6}$

Multi-channel photonic link at telecommunication band (1310nm or 1550nm) *for each fiber*

This requires microwave-to-optical transduction!

[1] Krinner et al., *EPJ Quantum Technology*, 6(1), p.2. (2019)
[2] S. Joshi and S. Moazeni, *Journal of Lightwave Technology*, (2024)
[3] Lecocq, F., et al. *Nature* **591**, 575–579 (2021).

Piezo -optomechanics

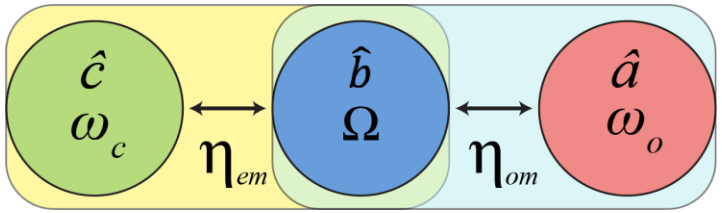

$$\hat{H}_{blue} = \hbar g(\delta\hat{a}\hat{b} + \delta\hat{a}^{\dagger}\hat{b}^{\dagger})$$

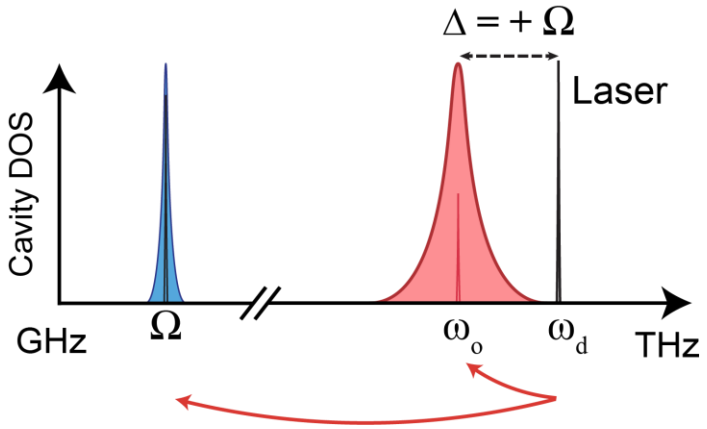

$$\hat{H}_{red} = \hbar g(\delta\hat{a}\hat{b}^{\dagger} + \delta\hat{a}^{\dagger}\hat{b})$$

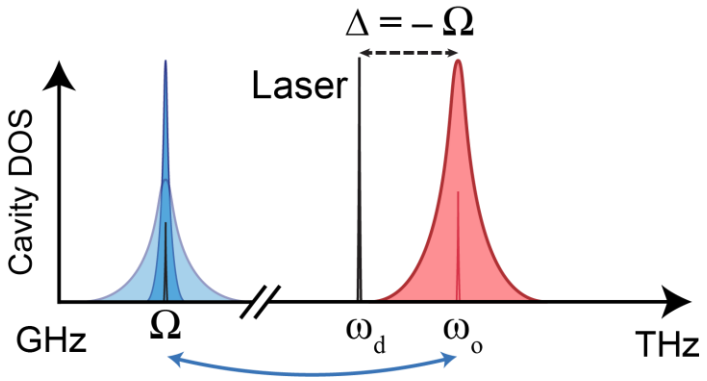

Electro-optics (EO)

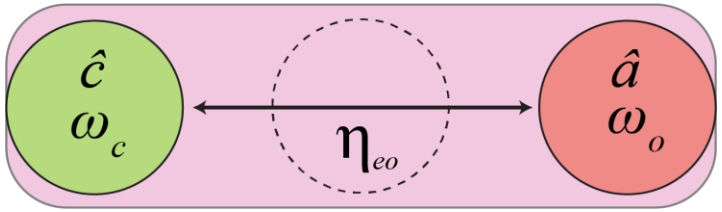

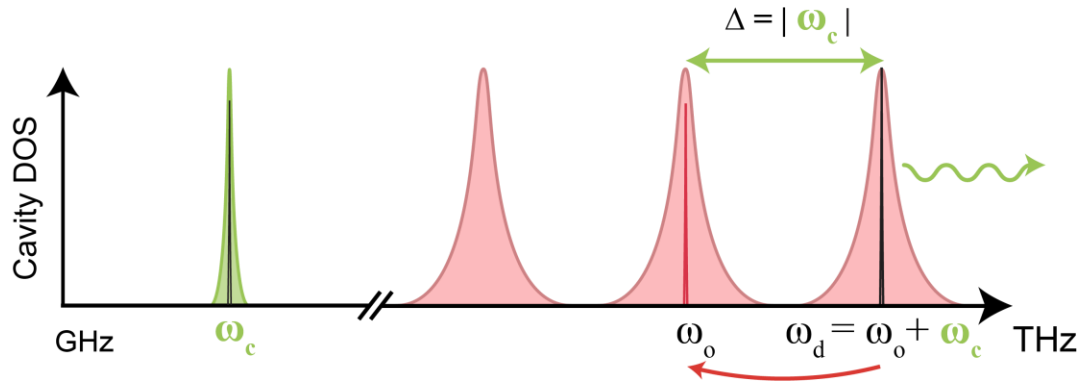

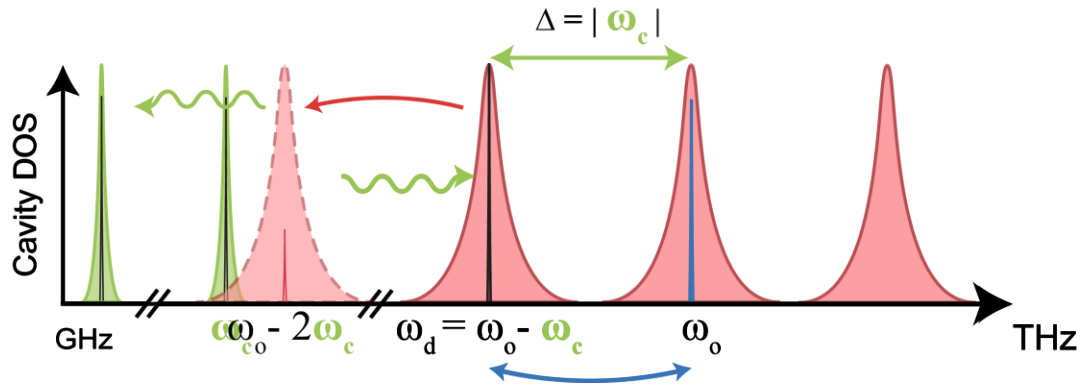

Parasitic down-conversion

Different material systems for microwave-optical transduction

Gallium phosphide (GaP) 1D OMC

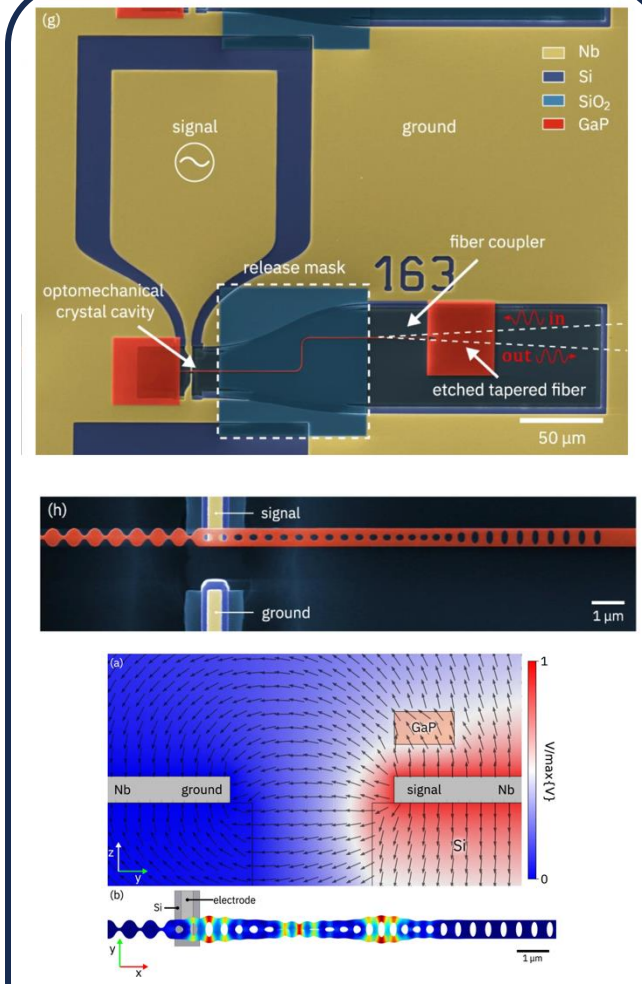

S. Hönl et al., Nat Comm (2022)

NbTiN on silicon (no piezo)

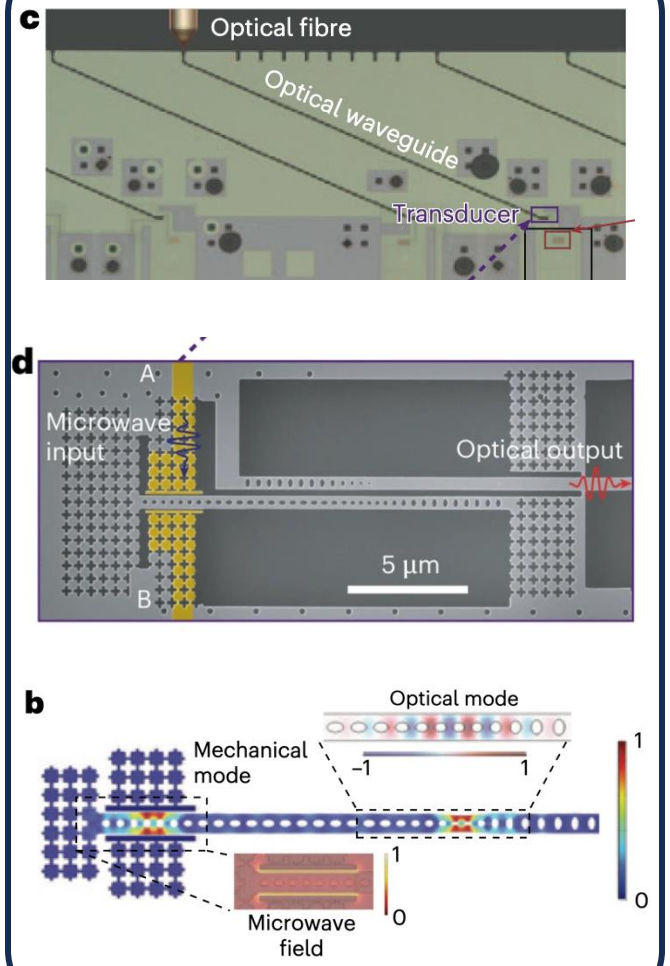

H. Zhao et al., Nat. Nanotech. (2025)

silicon (no piezo) 2D OMC

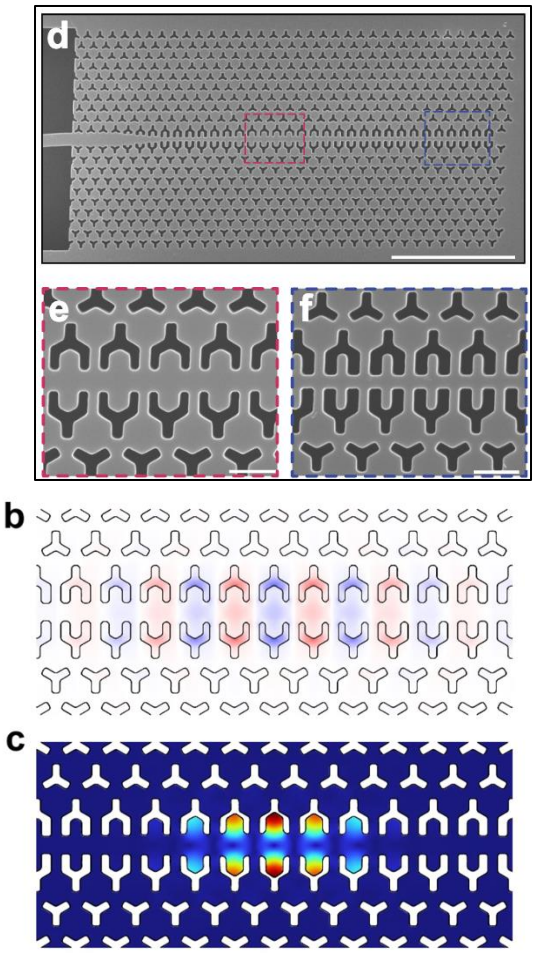

F.M. Mayor et al., Nat. Comm. (2025)

How to improve device scalability for integration?

Boron-doped Gallium Phosphide (BGaP)

- High refractive index $n \sim 3.1\ (1550\ nm)$
- High acousto-optic figure or merit $\mathcal{M}^{(2)}, \sim n^6$
- Slow acoustic speed $v \sim 4000\ m/s$
- Large second-order nonlinearity $\chi^{(2)} \sim 110 pm/V$
- Low piezoelectricity

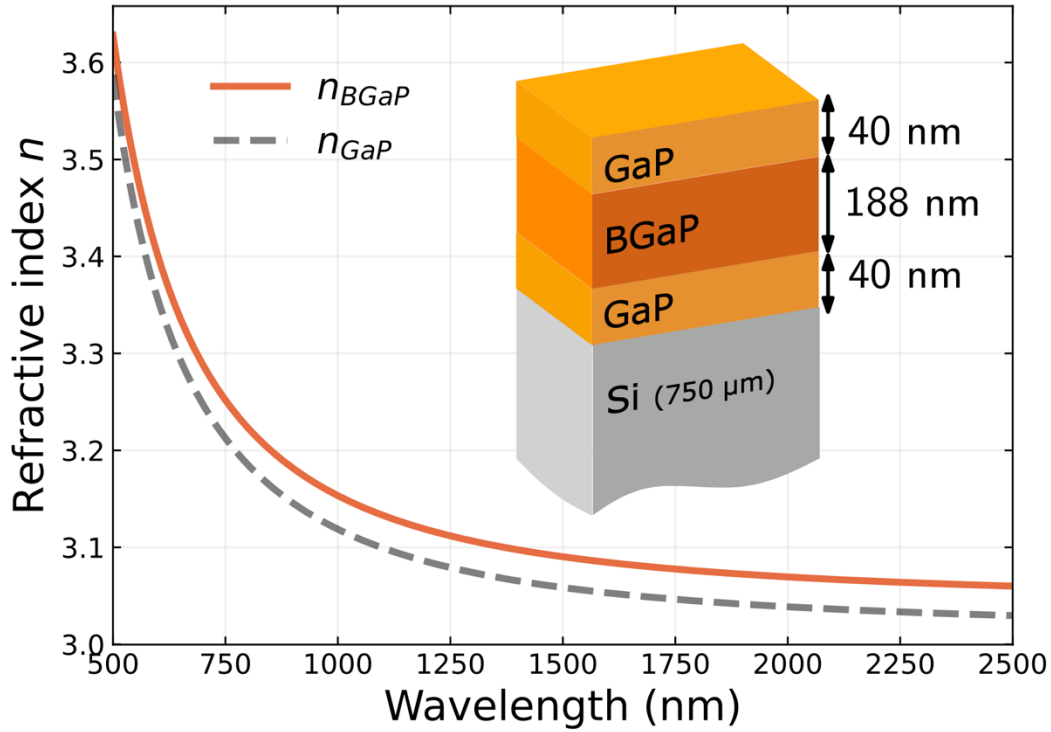

N. S. Yama*, I.-T. Chen* et al., Advanced Materials, (2023). *Equal contribution authors

Boron-doped Gallium Phosphide (BGaP): Acoustic Characterizations

Interdigital transducer (IDT)
on zinc oxide (ZnO)

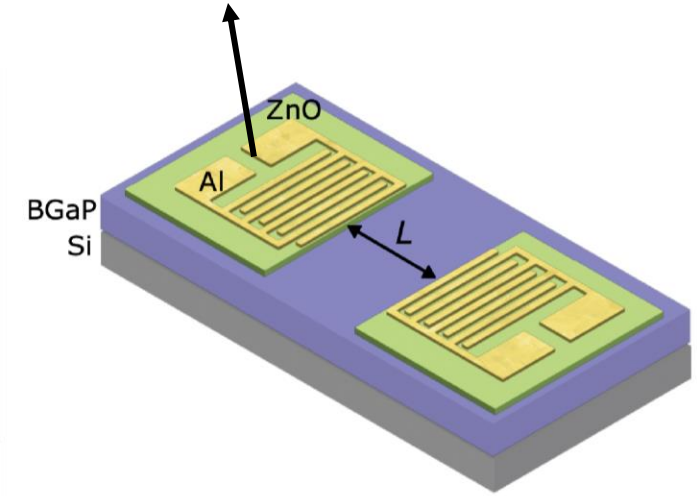

ZnO:
Strongly piezoelectric
Thin-film can be sputtered in house
Easy to integrate

High-order phononic mode

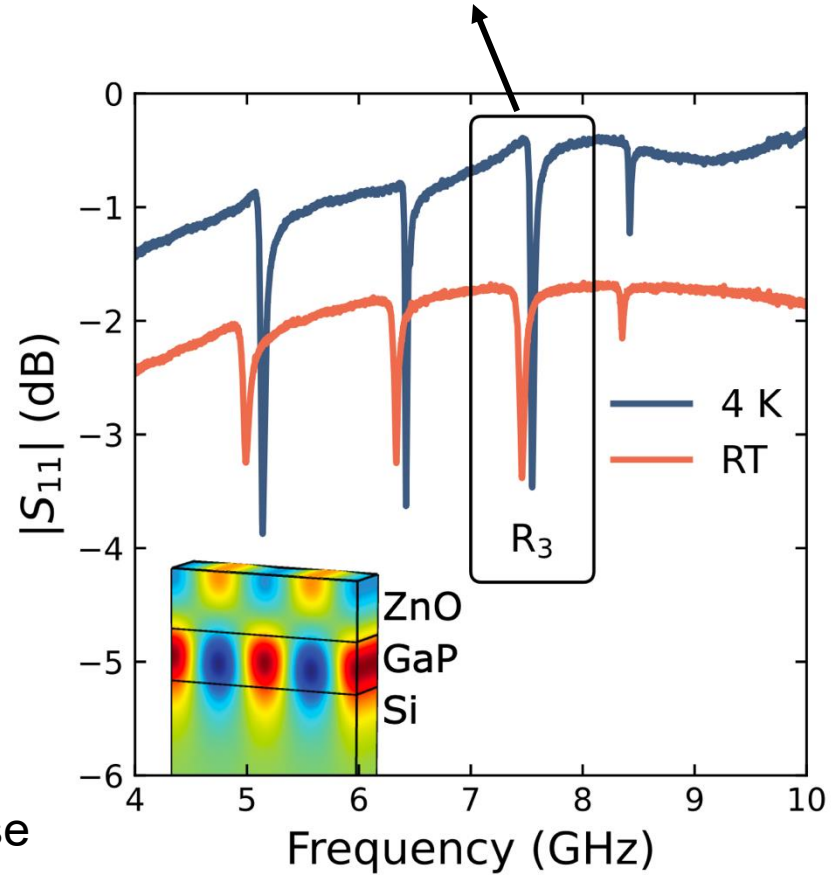

< 1dB/mm propagation loss at 4K

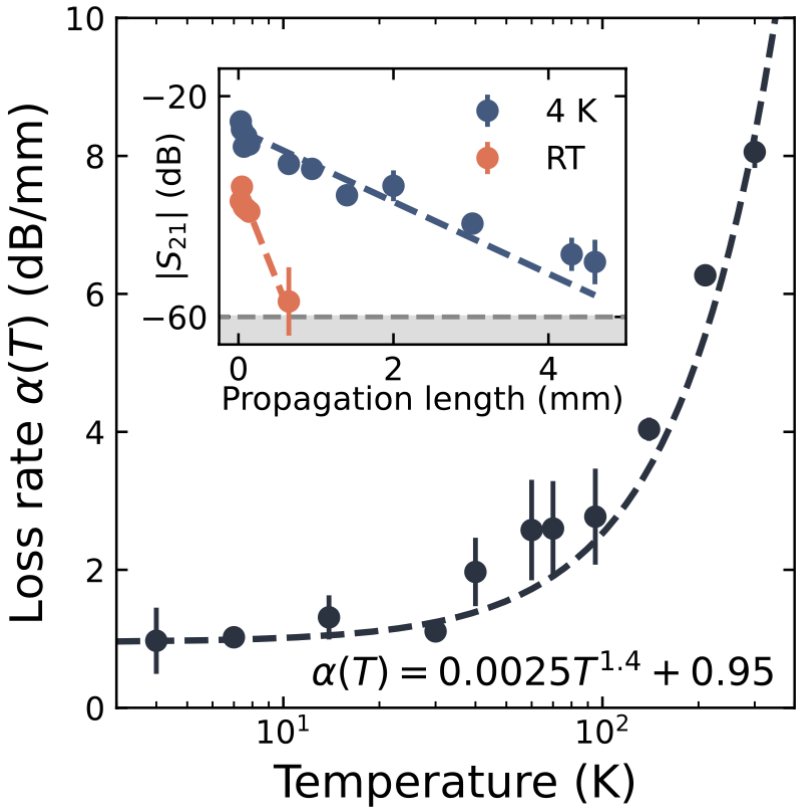

N. S. Yama*, I.-T. Chen* et al., Advanced Materials, (2023). *Equal contribution authors

Intermodal Brillouin Scattering

Microwave-to-optical transduction through intermodal Brillouin scattering

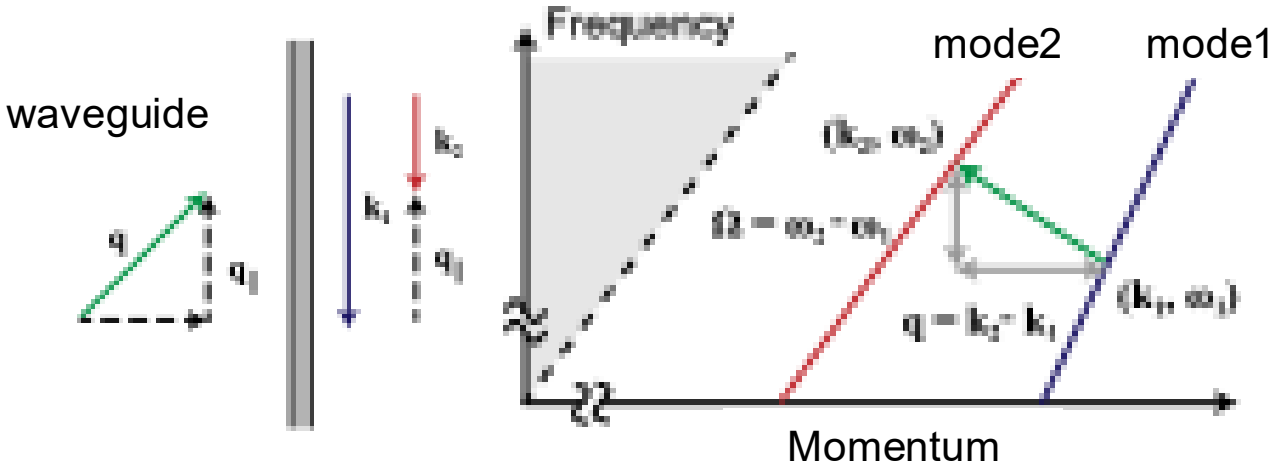

Type I: $q_\parallel = k$

Q. Liu, H. Li, and M. Li, Optica (2019)

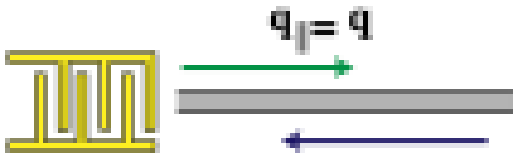

Type II: $q_\parallel = 0$

S. A. Tadesse and M. Li, Nat. Comm. (2014)

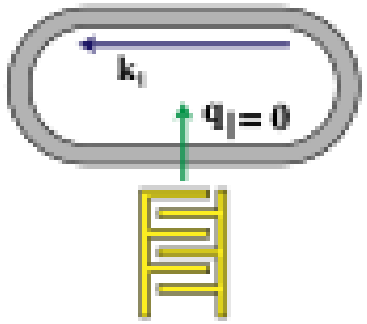

Type III: $q_\parallel \neq 0$

D. B. Sohn et al., Nat. Photonics (2018)

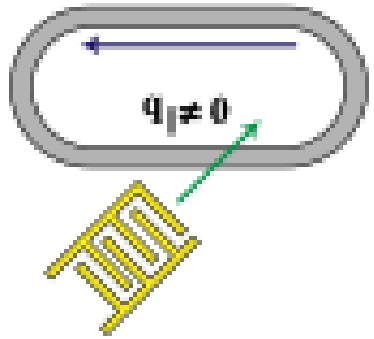

These do not utilize resonating phononic modes

Intermodal Brillouin scattering in waveguides

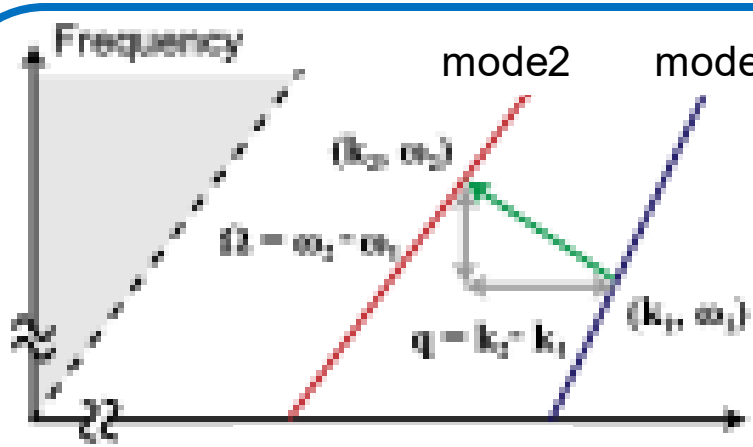

$$k_1 + q = k_2$$

+

Cavity-optomechanics

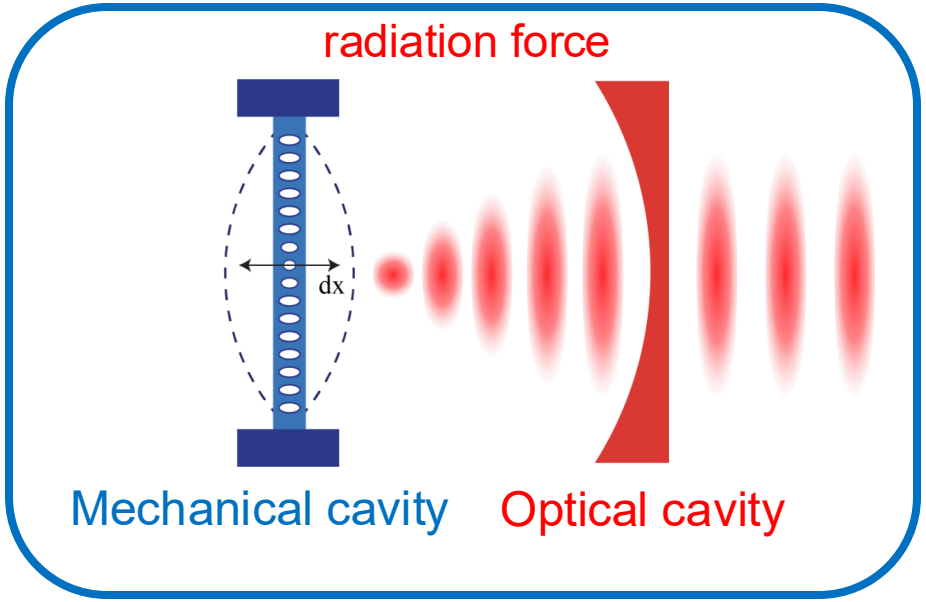

Type IV: Co-resonant phononic mode

Optomechanical integrated circuit (OMIC)

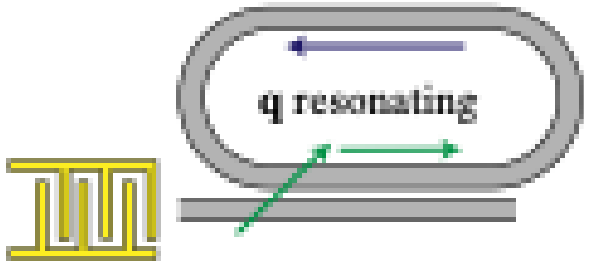

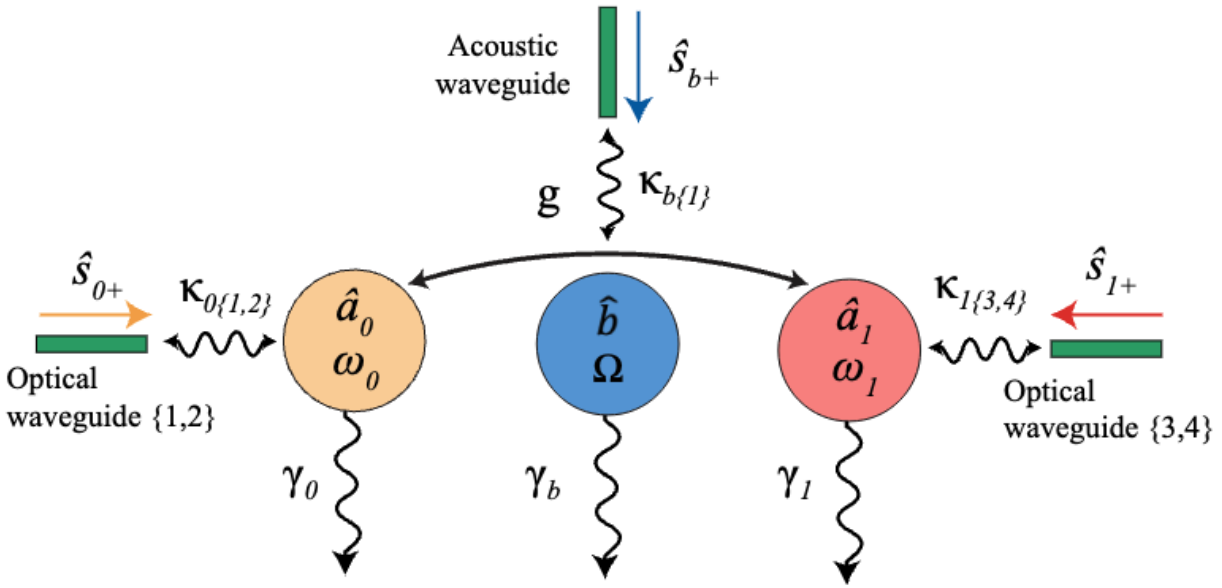

FIG. S1. **Overview diagram of the system model.**

EOM

$$\dot{\hat{a}}_0 = -i\omega_0\hat{a}_0 - ig_0\hat{a}_1\hat{b}^\dagger - \left(\hat{s}_{0+}\sqrt{\gamma_0} + \frac{\sqrt{\kappa_{0,1}\kappa_{0,2}}}{2}\hat{a}_0 + \frac{\sqrt{\kappa_{0,1}\kappa_{1,3}}}{2}\hat{a}_1\right),$$

$$\dot{\hat{a}}_1 = -i\omega_1\hat{a}_1 - ig_0\hat{a}_0\hat{b} - \left(\hat{s}_{1+}\sqrt{\gamma_1} + \frac{\sqrt{\kappa_{1,3}\kappa_{0,1}}}{2}\hat{a}_0 + \frac{\sqrt{\kappa_{1,3}\kappa_{1,4}}}{2}\hat{a}_1\right),$$

$$\dot{\hat{b}} = -i\Omega_0\hat{b} - ig_0\hat{a}_0^\dagger\hat{a}_1 - \left(\hat{s}_{b+}\sqrt{\gamma_b} + \frac{\gamma_b}{2}\hat{b}\right),$$

input-output theory

$$\hat{s}_{0,r-} = \hat{s}_{r+} + \sqrt{\gamma_{0,r}}\hat{a}_0,$$

$$\hat{s}_{1,r-} = \hat{s}_{r+} + \sqrt{\gamma_{1,r}}\hat{a}_1,$$

$$\hat{s}_{b,-} = \hat{s}_{+} + \sqrt{\gamma_b}\hat{b}.$$

I. -T. Chen et al., submitted (2025)

Summary and future directions

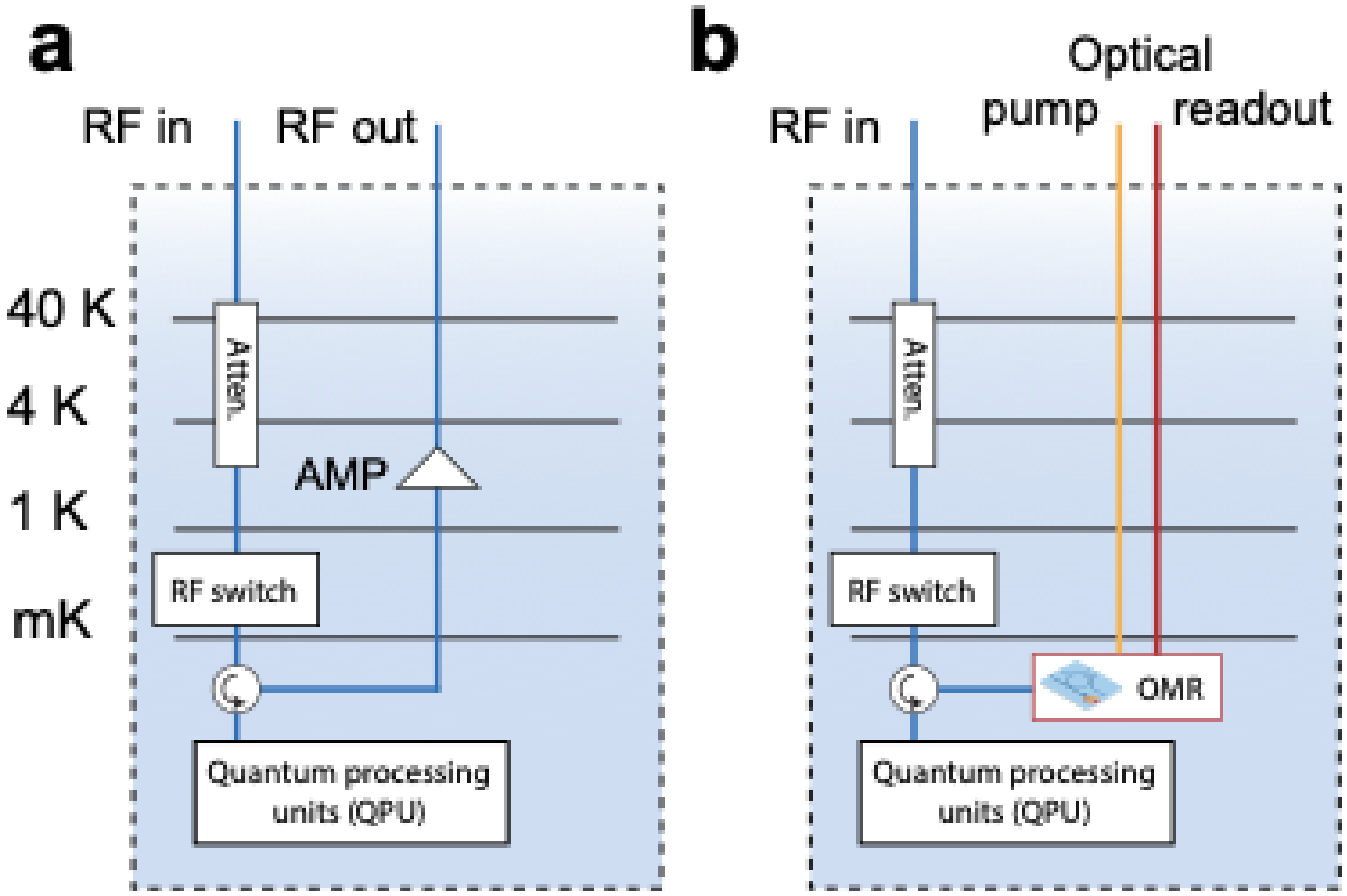

Non-volatile Tuning of Cryogenic Optical Resonators at 4K

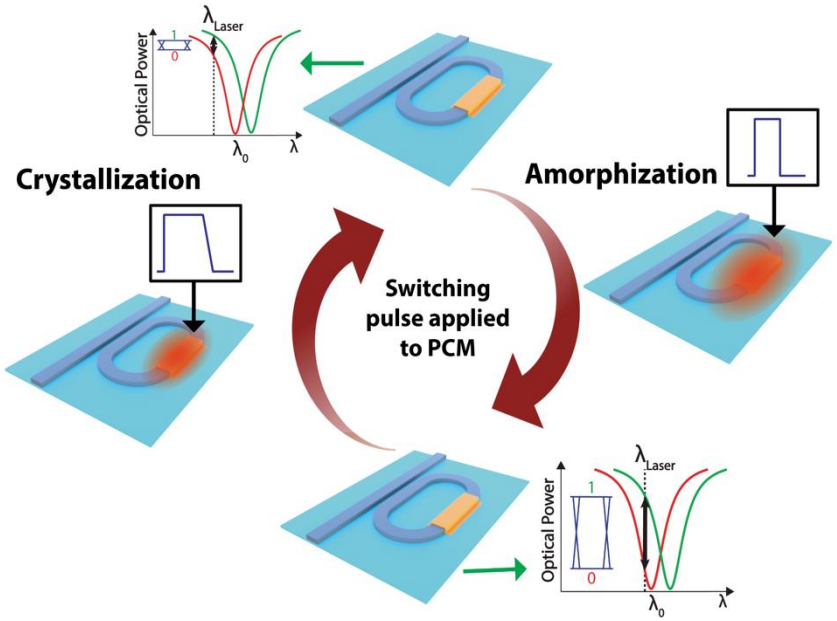

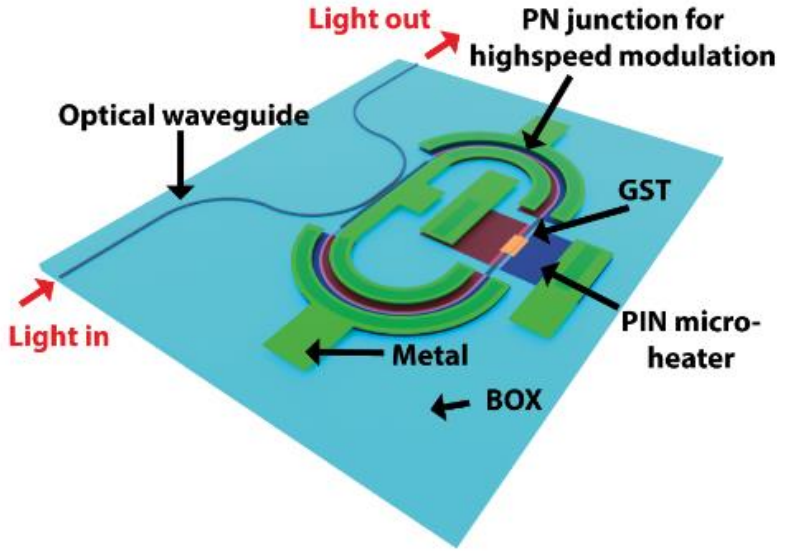

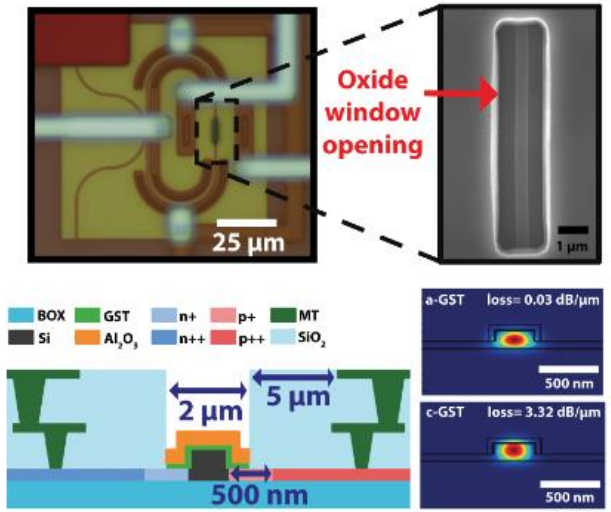

- Non-volatile phase-changing material (PCM)
- Set-and-forget. No DC bias required
- Commercial process taped out to AMF
- Post-process PCM-GST deposition in-house

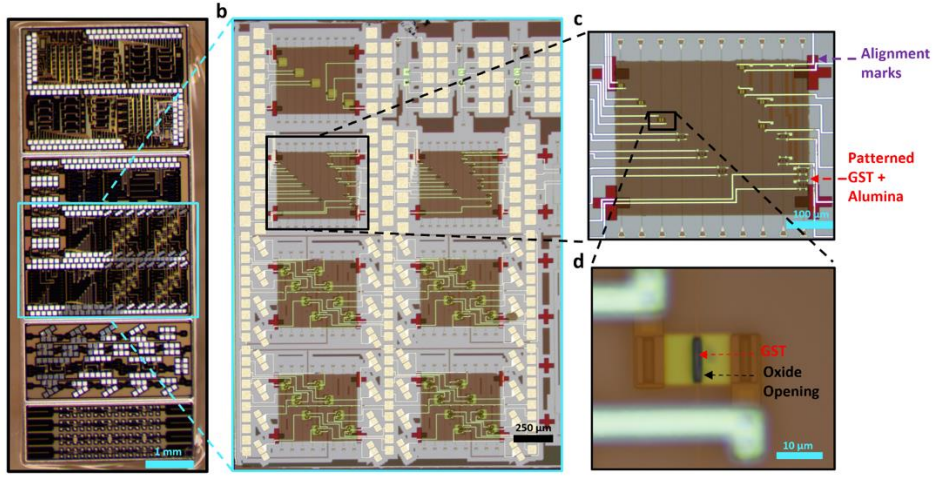

U. Adya, R. Chen, and **I. T. Chen** et al, arXiv:2410.08572v (2024)